Measurements of the Forces in Protein Interactions with Atomic Force Microscopy

Shiming Lin[1,3,*], Ji-Liang Chen[2], Long-Sun Huang[3] and Huan-We Lin[1]

[1]*Center for Optoelectronic Biomedicine,* [2]*Institute of Microbiology & Biochemistry and* [3]*Institute of Applied Mechanics, National Taiwan University, Taipei, Taiwan*

Abstract: Protein interactions with ligands or other proteins are controlled by a complex array of intermolecular forces. Although the interaction energies and intermolecular forces which contribute to the stabilization of the protein complex can be inferred indirectly from thermodynamic and kinetic approaches or be calculated with molecular simulation, recent progress in atomic force microscopy (AFM) has made it possible to quantify directly the ranges and magnitudes of the interaction forces between protein and other molecules. AFM has proved its value not only for resolving the topographical structure of protein samples, but also for probing the forces that control protein interactions or mechanical properties of proteins under physiological conditions. The objective of this review is to describe the uses of AFM in the determination of the forces that control biological interactions, focusing especially on protein-ligand and protein-protein interaction modes. We first consider measurements of the specific and the nonspecific forces that jointly control protein interactions. The review then indicates the theoretical background of AFM force curves and presents the great variety of force measurement modes that can be performed with this technique. In addition, some of the most recent studies in determining the unbinding forces and mechanical properties of proteins with AFM are reviewed and the available theoretical aspects necessary for the comprehension of the experiments have been provided.

Key Words: Protein interactions, atomic force microscopy.

1. INTRODUCTION

Long- and short- range interactions between biomolecules are central to the dynamic behavior of biological systems. The intermolecular forces which contribute to the stabilization of the protein-protein complex include hydrogen bonding, apolar (or hydrophobic), ionic (or coulombic) interactions and van der Waals interactions. These attractive forces share the commom property of being inversely proportional to the distance between the interacting molecules, e.g. van der Waals forces are inversely proportional to the sixth power of the distance between the molecules and electrostatic double-layer forces are inversely proportional to the square of this distance. Steric repulsion or the steric factor is a repulsive force involved in these interactions which is particularly sensitive to distance and is inversely proportional to the twelfth power of the distance between the interacting molecules. Any protein interaction will be governed by a superposition of some or all of these different forces for all atoms involved in the surface-protein interaction (Fig. **1**) (Israelachvili, 1992).

The qualitative aspects of the protein interactions with ligands or other proteins can be studied by the use of a variety of methods which utilize either thermodynamic or kinetic approaches. However, there is a little direct information about how the interaction energy between two structures is distributed in space because it is difficult to measure explicitly the interaction energy as a function of separation distance. The most direct way to obtain this kind of data is to measure the force (the derivative of energy with respect to distance) between two structures. Attempts to investigate the forces that characterize these interactions have been limited by the lack of suitable techniques to measure the forces between individual molecules. Several techniques have been developed for measuring forces between small structures, including mechanical springs made from glass fibers (Ishijima, *et al*., 1996; Nicklas, 1983), vesicle-based force transducers (Evans, 1995), optical tweezers (Svoboda, 1994) and the surface-forces apparatus (Israelachvili, 1992). Other approaches to investigate intermolecular forces include optical or diffraction methods to monitor the displacement of structures under a load resulting from osmotic (Parsegian *et al*., 1986) or hydrodynamic (Pierres *et al*., 1996) forces. These methods have sufficient sensitivity (0.01-1 nN) to detect the intermolecular forces operative in ligand-receptor binding but lack spatial resolution. Optical trapping (Kuo and Sheetz, 1993) is sufficiently sensitive but has a dynamic range that limits the breadth of the detectable force.

The atomic force microscope (AFM) was conceived as an instrument to image the surface structure of insulating samples (Binnig *et al*., 1986). This is achieved by scanning a probe attached to a cantilever over the sample and monitoring the deflection of the lever. By using a very sharp probe on a flexible lever, atomic resolution of surface structure is possible (Chen *et al*., 1992). AFM combines a high force sensitivity (theoretically 10^{-2} pN) (Lee *et al*., 1994a), a high dynamic range (0.001-5000 nN) (Dammer *et al*., 1995a), and a high positional accuracy (0.01 nm) with operational compatibility in physiological environments. The force sensitivity of the AFM also allows the spatial measurement

*Address correspondence to this author at the Center for Optoelectronic Biomedicine, National Taiwan University College of Medicine, 1-1 Jen-Ai Road, Taipei 100, Taiwan; Fax: +886-2-23949125; E-mail: sml@ntumc.org

1570-1646/05 $50.00+.00

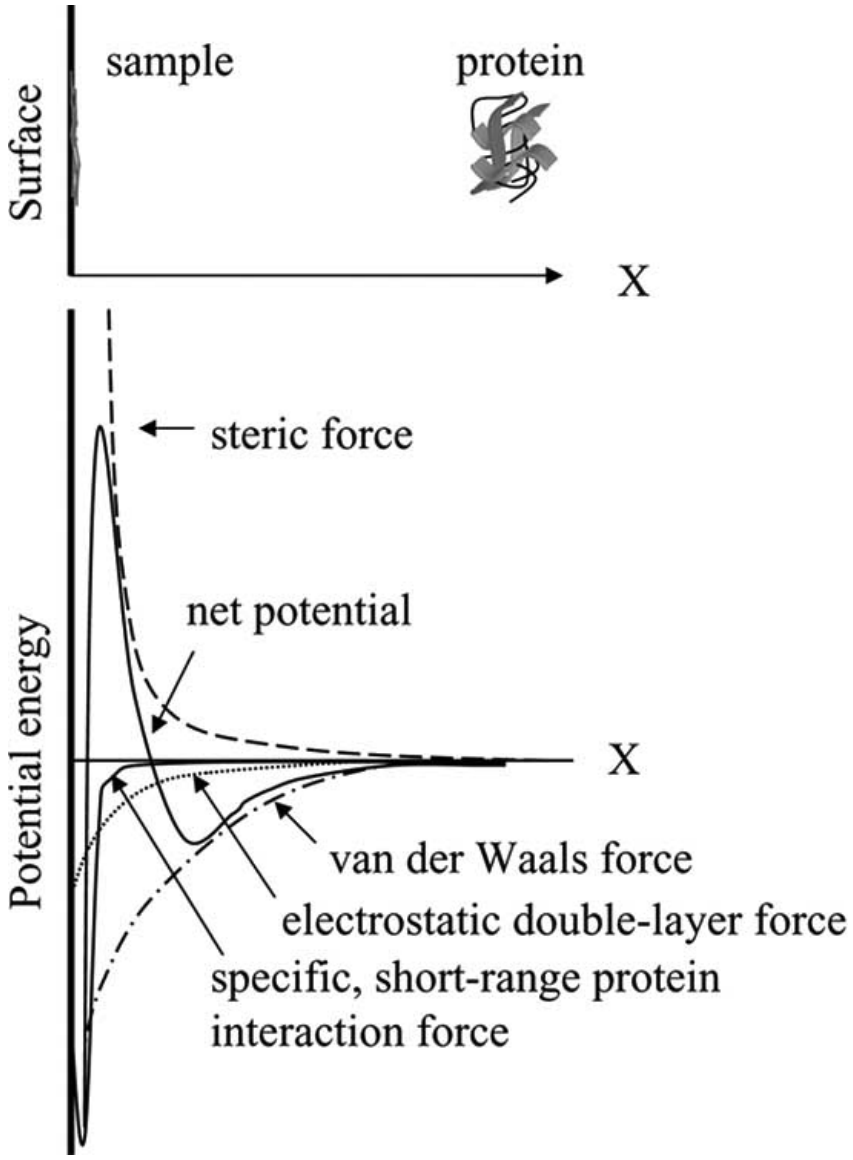

Fig. (1). Interaction potential between a soluble protein and a sample surface. X is the distance between two atoms. The net interaction force profile (or potential) is a superposition of the long-range van der Waals force, steric repulsion force, attractive or repulsive electrostatic double-layer force, and specific, short-range protein-ligand interactions.

of material properties, such as elasticity, adhesion, electrostaticity and viscosity of proteins and it is an extension of these property measurements which are used to measure molecular interactions. In a typical ligand rupture experiment, the protein is bound to a substrate surface and the ligand bound to the AFM probe. The ligand covered probe is brought into contact with the substrate and binding occurs. The probe is then withdrawn from the surface, pulling the ligand out of its binding pocket. The deflection of the lever, and therefore the force exerted on the probe by the protein / protein-specific ligand interaction, is recorded. The lever deflection is measured on approach to, and retraction from, the substrate surface. The difference between these two traces occurs through adhesion between the probe and surface and is attributed to the protein / ligand interaction. The maximum adhesive force measured is identified as the ligand unbinding force.

2. AFM FOR FORCE MEASUREMENTS

2.1. Instrumentation

Atomic force microscopy (AFM or scanning force microscopy) (Binnig *et al*. 1986) is a well known member of the so-called SXM family, where X stands for the physical principle behind a particular instrument, S for scanning and M for microscopy. The entire SXM technology is based on the invention of scanning tunneling microscopy (STM) by Binnig *et al*., (1982). In all these types of instruments, a sharp probe interacting locally with the specimen is scanned by a piezoelectric scanner, providing three-dimentional information about the surface. The resolution of these different techniques varies from submicrometers to about 0.1 nm and is critically dependent on the geometry of the tip and the nature of the interaction.

An atomic force microscope consists of four major components (Fig. **2**): (A) a cantilever deflection sensor, (B) a cantilever-mounted tip, (C) a piezoelectric micro-positioner, and (D) a digital control system.

(A) The most popular mode of detecting cantilever deflection, which is depicted in an instrument schematic in Fig. (**2A**), uses an optical lever and a quadrant, position-sensitive photodetector. This detection system can be used to follow the normal displacement (vertical motion) and the torsion (lateral motion) of the cantilever simultaneously. The photodetector is usually a simple photodiode, a semiconductor device which turns light falling on it into an electrical signal such that, as the incident light becomes brighter, the electrical signal increases. The photodiode is split into four sections enabling both vertical and lateral motions of the tip to be differentiated. By comparing the relative intensity of the reflected laser light in each quadrant, approximate quantification of tip displacement can be achieved. However for more precise measurement of tip displacement, as may be necessary if one is principally interested in performing force-distance spectroscopy on single molecules, linear position sensitive detectors are a better choice of detection method. (Pierce *et al*., 1994a).

(B) The heart of an AFM is the tip since this is the part which interacts with the biological sample. Quality and consistency are the key to good AFM tips. Modern AFM tips and cantilevers are made by microfabrication using many of the techniques that have been developed for integrated circuit manufacture, such as lithographic photo-masking, etching and vapour deposition. Cantilevers and tips are nearly always made from either silicon, silicon nitride (Si_3N_4), or diamond. They can be conducting or non-conducting, and are often coated with another material. When optical sensing methods are used to monitor cantilever deflection, they are usually coated with a thin gold layer to improve their reflectivity or, if magnetic sensitivity is required, a ferromagnetic coating may be applied. Since normal spring constants (*k*N) for cantilevers are 0.01-100 N/m and instrumental sensitivities for normal deflection are 0.01 nm, the corresponding limits in force detection are 10^{-13}-10^{-8} N (Burnham and Colton 1993). These limits reflect a combination of the thermal excitation of the cantilever as well as optical and electrical noise.

(C) Modern AFMs use one of two basic types of scanner mechanisms: there are some that scan the sample, and others that scan the tip. However, both rely upon piezoelectric transducers. The most frequently used driver is a hollow-tube scanner, which can move the tip or sample in all three mutually perpendicular directions (Morris *et al*., 1999). The scanner consists of a thin-walled hard piezoelectric ceramic which is radially polarized. Electrodes are attached to the internal and external faces of the scanner tube, and the external face of the tube is split into quarters parallel to the axis. By applying a bias voltage between the inner and all the outer electrodes, the tube will expand or contract, i.e. move in the *z* direction. If a bias voltage is applied just to one of the outer electrodes the tube will bend i.e. move in the x and y directions.

(D) The digital control system used in modern AFMs consists of four elements which are illustrated in the schematic diagram shown in Fig. (**2A**). The first is the digital control electronics, often present in the form of a digital signal processor (DSP) card, which performs all of the signal processing and calculations involved in operation of the AFM in real-time. The DSP linked to the second element of the electronics, a translator box which performs the conversion of the digital signals sent from the DSP card to an analogue form to run the microscopes' scanner mechanism. The third part of the control electronics is the high voltage (HV) amplifier. It amplifies this low voltage signal to produce a high voltage signal, typically ± 150V, that drives the piezoelectric scanner. The final pieces of the system are the laser driver electronics and the raw data signal pre-amplifier. The laser driver circuitry provides power for the AFMs' laser and has its own feedback loop which varies the laser power supply to maintain a constant laser intensity. For the optical beam method used by most AFMs, in addition to simple amplification, the control electronics, also has a series of summing and difference amplifiers to produce an output signal for the translator box which defines either vertical or lateral motion of the AFM tip (Fig. **2B**).

2.2. Principle of Operation

The force between the tip and the sample varies as the biological sample is scanned beneath the tip. Changes in force are sensed by the tip, which is attached to a flexible cantilever. The deflection of the tip is a measurement of the forces sensed by the cantilever. Because the spring constant of the commonly used cantilever (0.1 to 0.01 N/m) is much smaller than the intermolecular vibration spring constant of the atoms in the specimen (10 N/m), the cantilever can sense exquisitely small forces exerted by the individual sample atoms. The sensed forces are then transduced to generate molecular images. Depending on whether the cantilever is sensing repulsive or attractive forces, different imaging modes can be applied. The operation of the AFM depends on monitoring forces between tip and sample and in this section, the different operation modes likely to be encountered in protein interactions will be described.

2.2.1. Contact Mode

The most popular instrumental mode of the atomic force microscope is the contact mode (Fig. **3A**), where the tip is brought into physical contact with the sample, and the sample is scanned beneath it (the tip-sample interaction is repulsive in nature). This process can be performed either in air or under a liquid, such as a biological buffer. The value of the pre-set imaging force is adjusted in the instrument software, which is equivalent to performing the entire scan with the cantilever bent by a small but fixed amount – hence this is known as 'constant deflection mode' (also called 'constant force mode'). In the variable deflection mode (constant height mode), the feedback loop is open, such that the cantilever undergoes a deflection proportional to the change in the tip-sample interaction, i.e., the force sensed by the cantilever. The surface image is then constructed from the deflection information. This mode is usually unsuitable for a sample with large surface corrugation (e.g., cell surface), because the force fluctuations and thus the deflections of the cantilever are enormous, resulting in tip-sample disengagement.

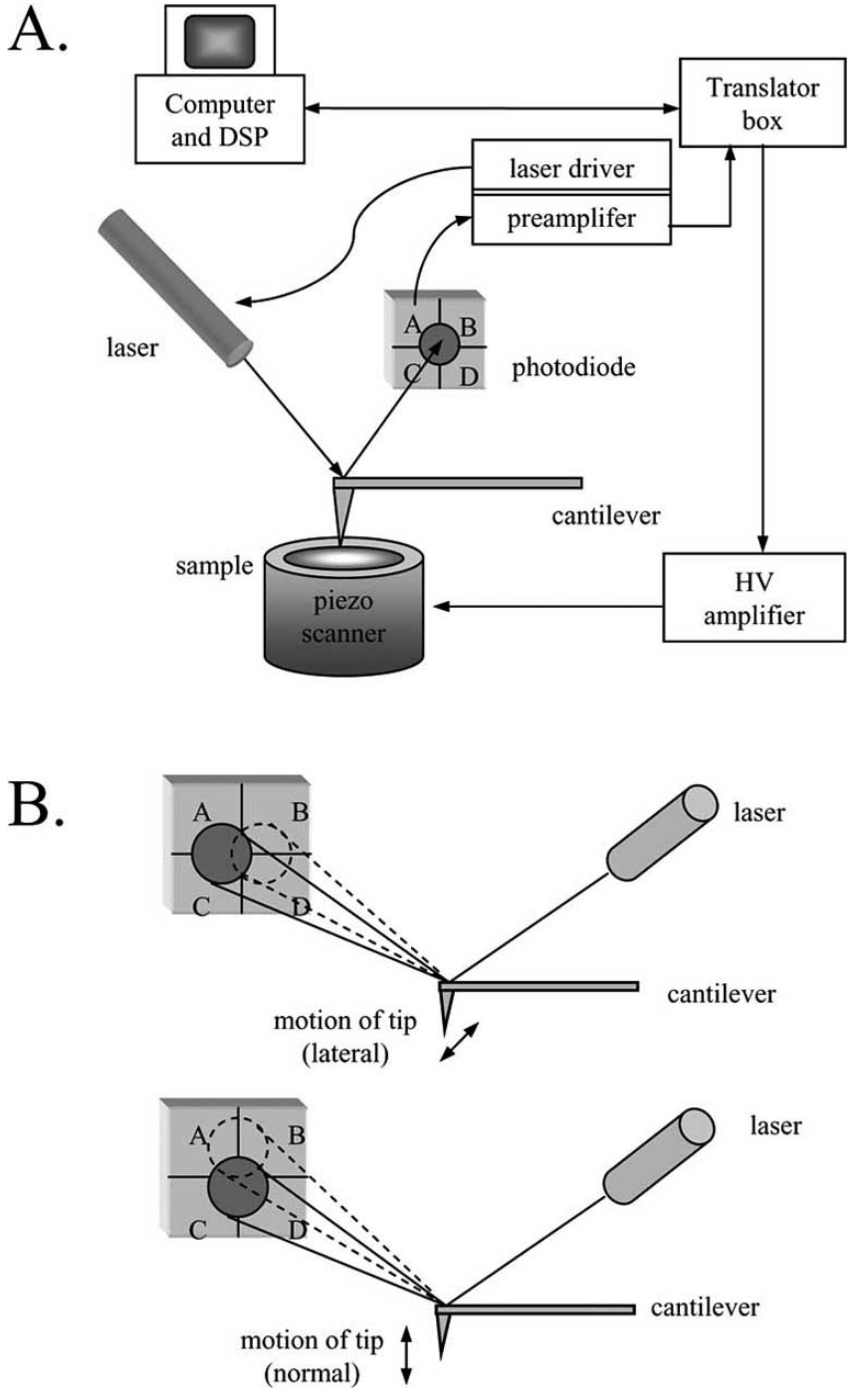

Fig. (2). Schematic representation of the atomic force microscope. (A) Typical AFM control system broken into main components. (B) By splitting the photodetector into four segments, lateral motion or twisting of the cantilever (top) can be distinguished from normal or vertical motion (bottom).

2.2.2. Tapping Mode

For soft materials such as protein molecules, the application of even the smallest force in the contact-mode AFM mode might damage the weak surface structures. One of the factors causing this problem is the lateral force that the tip applies to the sample surface. To avoid this lateral force, one can employ tapping-mode AFM in air or under liquid, in which the cantilever is oscillated at very high frequency as it scans the biological sample (Fig. **3B**). In this mode, a relatively stiff and beam- type cantilever is used when the instrument is operated in air. The purpose of using this mode is to prevent the AFM tip from being trapped by the 'capillary force' caused by the extremely thin film of water surrounding samples in air. Here the cantilever is deliberately excited by an electrical oscillator to amplitudes of up to approximately 100 nm, so that it effectively bounces up and down (or taps) as it travels over the sample. The deviations in oscillation amplitude associated with sample surface

corrugations, are used as signals for image formation. This ensures a much shorter tip-sample contact time and smaller lateral forces exerted on the cantilever. In liquid tapping mode there is no capillary force to cause imaging difficulties because the sample is immersed under a liquid, so a super stiff cantilever is not required. In this mode the cantilever can be excited by applying a small sinusoidal electrical signal onto the z-channel input of the high voltage amplifier. This causes the main piezoelectric tube to vibrate up and down in the vertical (z) direction, while still performing its normal task of responding to signals from the control loop. Therefore the sample, and the liquid surrounding it, begin to vibrate. This vibration is also communicated to the cantilever, which is immersed in the liquid, by viscous coupling. The disadvantage of this mode of operation is that the vertical imaging force can be large, increasing the possibility of protein sample damage.

2.2.3. Force-Modulation Mode

In contrast to the tapping mode, in which the amplitude of the vibrating cantilever is in the 20-100 nm range, the force-modulation technique uses a much smaller amplitude to prevent tip-sample disconnection (Fig. **3C**). Also, in force-modulation mode, the vertical position of the sample is modulated with much smaller amplitude to avoid breaking contact with the tip. The resulting deflection of the cantilever is then correlated with the elasticity of the tip-sample microcontact, noting that the oscillation can be modulated with a preselected amplitude and frequency depending on the elasticity and viscoelasticity of the sample. For direct determination of the sample stiffness in the tip-sample contact area, it can be more convenient to apply the force to the tip rather than modulating the vertical position of the tip or sample. This can be achieved by coating the tip with magnetic material and applying an external magnetic field to produce a modulation of the force on the sample surface. The frequency of the force modulation employed varies from 10 Hz to 20 kHz (Radmacher *et al*., 1992).

2.3. Forces in AFM

As the name 'atomic force microscopy' suggests the important interactions between the tip and sample are due to one or more forces. The sum of the forces that acts on the tip causes the deflection of the cantilever; these forces can be attractive and/or repulsive. The forces acting on the tip vary, depending on the mode of operation and the conditions used for imaging. The different types of forces likely to be encountered in protein interactions will be described in this section.

2.3.1. Force-Distance Curves

In the common mode of operation, the feedback loop of the AFM operates to maintain a constant cantilever deflection, and images are nominally acquired at constant force. The assumption is that locally the force-distance curve is the same and hence, at constant cantilever deflection (assumed constant forces), the image is determined solely by the topography of the sample surface. If the force-distance curves vary between the substrate and sample, or locally across the sample, then the image contrast is not simply a reflection of the sample topography, but also depends on material properties. Fig. (**4**) illustrates a variety of types of force-distance curves, which may be observed for protein interaction systems.

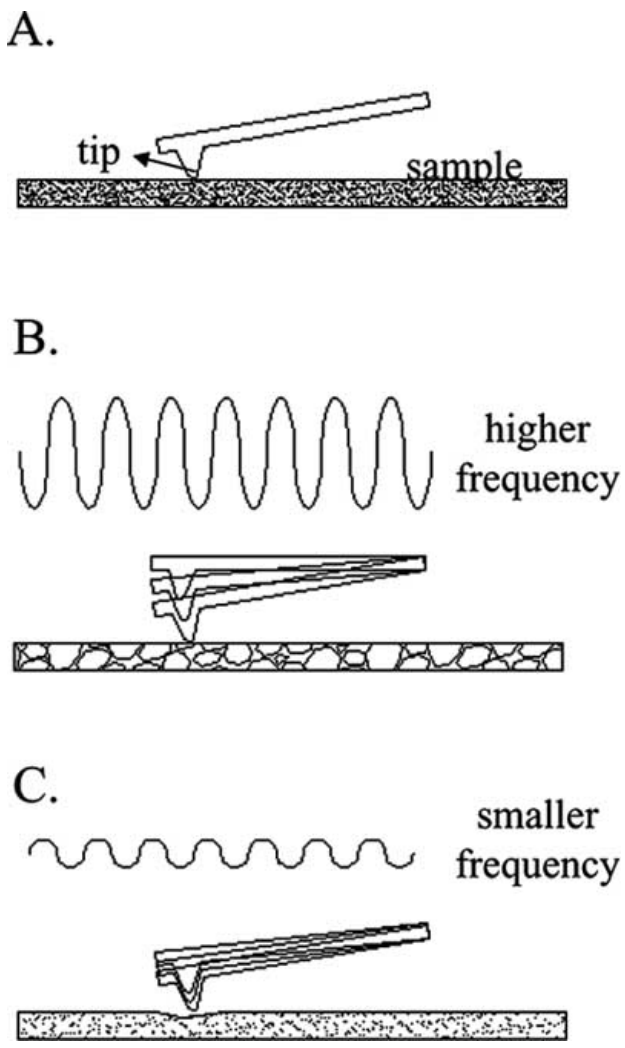

Fig. (3). Tip-sample arrangements in the three modulation modes of AFM. (A) Contact mode detects topography, elasticity, adhesion, and friction of a sample; (B) Tapping mode is sensitive to topography and adhesion force of the sample; (C) Force-modulation mode is responsive to the elasticity and viscosity properties of the sample.

2.3.2. Van Der Waals Force

It is possible to characterize both attractive and repulsive parts of the force-distance relationship between the atoms in the sample and those found in the very end of the pyramidal AFM tip by modeling the interaction. This involves the variation of the potential energy of one particle, say at the apex of the AFM tip, due the interaction with a particle at the surface of the sample. As their separation distance (z) changes, so does the value of the potential energy, which can be described mathematically by the pair-potential energy function $E^{pair}(z)$. A special case of the well known 'Mie' pair-potential energy function is used to model this behaviour (Morris *et al*., 1999),

$$E^{pair}(z) = 4\varepsilon\left[\left(\frac{\rho}{z}\right)^{12} - \left(\frac{\rho}{z}\right)^{6}\right] \quad [1]$$

where ε and ρ are constants that depend on the material.

Incidentally, ρ is approximately equal to the diameter of the atoms involved, and is sometimes called the hard sphere diameter. Eq. [1] illustrates the variation of the pair-potential energy between two atoms. The $1/z^{12}$ term accounts for the steep increase in E^{pair} (z) at small separations i.e. when z < ρ where the atoms strongly repel each other due to the Pauli exclusion principle. The $1/z^{6}$ term is responsible for the slower change in the attractive behavior at relatively large separations, where the van der Waals force dominates.

2.3.3. Adhesive Force

Obviously AFM tips do not last forever. With time they become blunt and contaminated with small amounts of the sample. The effect leads to a greater contact area between tip and sample, and ultimately to the presence of what is commonly known as an 'adhesion force'. This is a major problem when studying small molecules since they are easily damaged by high forces. However, it is not so critical when studying large objects such as protein macromolecules because they can invariably withstand higher imaging forces. Fortunately, it is possible to check for the presence of adhesion by generating a force-distance curve, and examining it for any asymmetry in its inward and outward portions, as displayed in Fig. (**4A** and **4C**). The curve on Fig. (**4C**) shows the presence of a strong adhesion force whereas the curve in Fig. (**4E**) is reasonably ideal for most imaging situations.

2.3.4. Capillary Force

A typical AFM tip has a radius of curvature of around 20 nm. When resting on a surface it will act as an ideal nucleation site for the condensation of water vapour present in the air. In addition, a layer of water will condense on the sample surface at normal relative humidity. This means that when imaging in air the tip will be pulled down towards the sample by a strong liquid meniscus, giving rise to the so-called 'capillary force' (Fig. **4C**), which glues the tip to the sample. Depending on the geometry of the tip and the relative humidity, this capillary force can be quite large. For a tip radius of R, the capillary $F_{ad,}$ can be calculated according to the equation (Israelachivili, 1992; Shao *et al*., 1996)

$$F_{ad} = 4\pi\gamma R$$

where γ is the surface tension of water and R is the radius of curvature of the tip. One should note that the derivation of equation [1] is based on the assumption that the water layer has a finite boundary. The validity of this assumption for AFM imaging is not clearly demonstrated, since such a water layer is actually continuous on hydrophilic surfaces under intermediate humidity (Guckenberger *et al*., 1994; Shao *et al*., 1996).

2.3.5. Electrostatic Force

The electrostatic interaction force between a charged surface and a dielectric tip has been systematically studied by Butt (1991a, b; 1992) using numerical calculations and experiments with tips of silicon nitride, glass and diamond. The electrostatic force is another long-range interaction which could have an appreciable magnitude. Depending on the charges involved, it can be either attractive or repulsive, and the strength can be varied by the ionic strength of the solution. This is perhaps most relevant for the imaging of protein molecules (Philippsen *et al*., 2002), because protein surfaces can often carry charges depending on the residues exposed and the local pH (Melander and Horvath, 1977). Even if the tip does not carry charge, the difference between the dielectric constants of the tip and the solution can still result in a measurable force if the sample is charged (Fig. **4B**). Generally, the greater the ionic strength of the imaging medium, the lower the electrostatic repulsion that an approaching AFM tip experiences. Therefore, it is possible to electrically shield the AFM tip from the influence of the relatively large forces present when imaging in some liquids, such as buffers. This is usually achieved by adding a small quantity of a salt, containing divalent metal ions, to the imaging liquid.

2.3.6. Elastic Force

In AFM, an indentation experiment is done by employing the force curve mode in which the deflection of the cantilever is plotted as a function of the z height of the sample. On a stiff sample, the deflection is either constant as long as the tip is not in contact with the sample or proportional to the sample height while the tip is in contact, as shown in Fig. **4A**. With soft biological samples, e.g., proteins, the tip may deform (compress) the sample when the loading force is increased (Tao *et al*., 1992; Samori *et al*., 1993; Radmacher *et al*., 1995; Radmacher 2002). Thus, the movement of the tip will be smaller than the movement of the sample base, the difference being the indentation of the protein sample (Fig. **4B**) (Radmacher *et al*., 1994 1995; Vinckier *et al*., 1996; Domke and Radmacher, 1998). In this case, the cantilever deflection will be dependent on the viscoelastic properties of the sample and this will contribute to contrast in the image. On a positive note, this effect permits the mapping of the mechanical properties of the sample.

2.3.7. Unbinding Force

The unbinding force of ligand-receptor interaction can be measured by employing the force-distance curve of AFM. In some cases, the resultant retraction force curves have jagged appearance (Fig. **4D**), which is thought to correspond to multiple pairs unbinding at different times. Controls include competition with excess free ligand/receptor to occupy all available sites and the use of nonspecific ligands. At a fixed lateral position, a cantilever carrying a ligand is moved toward a probe surface to which receptors are attached and subsequently retracted. The cantilever deflection d is measured independent of the tip-surface Δ z. The force F acting on the cantilever directly relates to the cantilever deflection d according to $F = k\ d$, where k is the cantilever spring constant. During the tip-surface approach, the cantilever deflection remains at zero far away from the surface because there is no detectable tip-surface interaction. At a sufficiently close tip-surface separation, the ligand on the tip has a chance to bind to a receptor on the surface. If ligand-receptor binding has occurred, an attractive force develops (unbinding event) upon retraction and increases with increasing tip-surface separation. The physical connection between tip and surface sustains the increasing force until the ligand-receptor

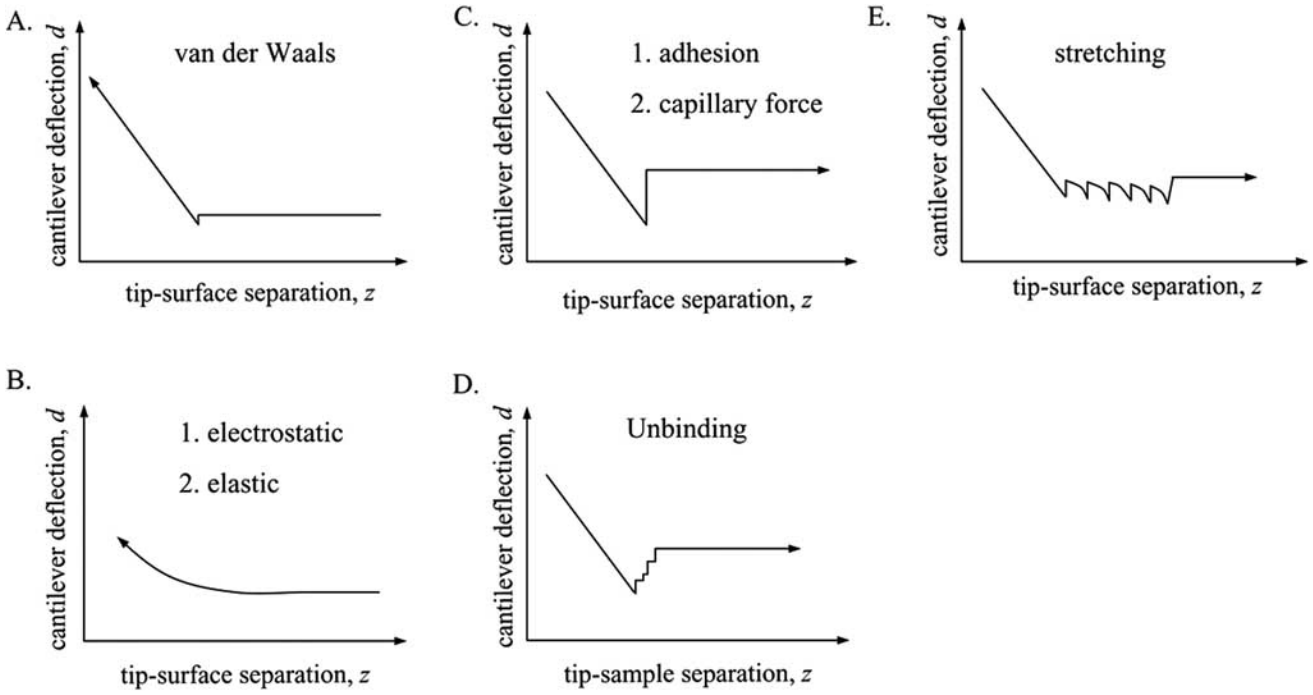

Fig. (4). Schematic diagram illustration of the force-distance curves of cantilever deflection '*d*' versus tip-sample separation '*z*' observed for protein samples. Curves (A, B) are approach curves and curves (C, D, E) are retraction curve, as indicated by the arrows. (A) An ideal, attractive, van der Waals force in the absence of other forces. (B) Repulsive electrostatic double-layer force in liquid or the indentation curve on an elastic sample. (C) Adhesive interactions in the absence of contaminating adsorbates (adsorbed impurities) or capillary force resulting from the formation of a water bridge between the tip and sample. (D) The sequential unbinding of specific multiple protein-ligand pairs. (E) Polypeptide chain stretching force curve resulting from the multi-domain proteins break or detach from the surface.

complex dissociates and produces a stepwise return to zero deflection from the point of maximal adhesion. This is thought to be due to the sequential unbinding of multivalent receptor-ligand pairs.

2.3.8. Stretching

A different form of 'adhesion' occurs when a polymer is captured between the AFM tip and the substrate. In this case, there is a very distinctive 'adhesive' force as the tip is pulled away. Typically, these curves initially retrace the approach curve near the surface but, away from the surface, exhibit a smooth negative deflection as the polymer is stretched until it breaks or detaches from the tip or the substrate, and the cantilever returns to the zero-deflection line (Fig. **4E**). If multiple polymer molecules, e.g., multi-domain proteins, attach to the tip and substrate, a saw-tooth pattern can be observed as individual polymers detach. There are several modes, such as the worm-like or freely-jointed chain models, that can be used to describe the force-distance relationships for extending polymers. Stretching measurements of high molecular weight multi-domain protein polymers show force-distance relationships in agreement with the worm-like mode (Rief *et al*., 1997).

3. MEASUREMENTS OF PROTEIN INTERACTION FORCES

3.1. Introduction

A major drawback of the AFM is its inability to chemically identify the molecules of the specimen. One of the possible approaches to solving this problem is to analyze the experimentally measurable forces acting between the AFM probe and the surface of the specimen. These forces can be mapped during approach and retraction between the AFM probe and the specimen surface. The adhesion contact forces between the AFM probe and substrate surfaces have already been reported in earlier literature (Ducker, *et al*., 1992; Mizes *et al*., 1991; Creuzet *et al*., 1992). Such adhesive forces are nonspecific and can be directly related to the interfacial energy between the AFM probe and the specimen.

In contrast to nonspecific forces, protein molecules primarily interact through specific molecular forces. Recently, the molecular interaction forces between protein-specific ligands and surface-bound proteins have been measured using the AFM technique, as seen in Table **1**. The forces required to separate a ligand from its specific binding site are different from the forces needed to remove a nonspecifically bound ligand (Pierce *et al*., 1994b). Since the AFM can measure these differences of the specific adhesion forces in a spatially resolved manner, this "specific adhesion force contrast" can be used to identify binding molecules and determine their distribution on the surface of the specimen. When the specificity of protein interactions results in a force contrast, one can separate topographical and chemical surface information. In biological systems, where the molecular recognition events determine the specificity of interactions, the force contrast could be used to identify and map the distribution of those surface-immobilizated proteins which are capable of binding AFM tip-bound ligands. In this

Table 1. Protein Interaction Forces

Molecular partners	On substrate	On AFM tip	Average forces (pN)	Reference
Avidin/biotin systems				
Avidin/biotin	Biotin	Avidin	160 ± 20	Florin *et al*. (1994)
Biotin/streptavidin	Streptavidin.	Biotinylated BSA	340 ± 120	Lee *et al*. (1994a)
Avidin/biotin	Biotin	Avidin	15000 ~ 20000	Moy *et al*. (1994b)
Avidin/iminobiotin	Avidin	Iminobiotin	85 ± 10	Moy *et al*. (1994a)
Streptavidin/biotin	Streptavidin	Biotin	257 ± 25	Moy *et al*. (1994a)
Biotin/streptavidin	Streptavidin	Biotinylated BSA	100 ~ 450	Chilkoti *et al*. (1995)
Biotin/streptavidin	Streptavidin	Biotin	300	Allen *et al*. (1996)
Biotin/streptavidin	Streptavidin	Biotin	~ 200	Wong *et al*. (1998)
Streptavidin/Biotin	Biotin	Streptavidin	126 ± 2.3 and 207 ± 5.8	Yuan *et al*. (2000)
Antigen/antibody (Ag/Ab)				
Protein G /IgG-Ab	Protein G	IgG-Ab	3000 ~ 4000	Moy *et al*. (1994b)
Fluorescein/anti-fuorescyl Ab	Anti-fuorescyl Ab	Fluorescein	200	Stuart and Hlady (1995)
Human serum albumin (HSA)/ anti-HSA Ab	HSA	Anti-HSA Ab	244 ± 22	Hinterdorfer *et al*. (1996)
Biotinylated BSA / anti-biotin Ab	Anti-biotin Ab	Biotinylated BSA	111.5 ± 98.6	Dammer *et al.* (1996)
Ferritin/anti-ferritin Ab	Anti-ferritin Ab	Ferritin	49 ± 10	Allen *et al*. (1997)
Intercellular adhesion molecule-1 (ICAM-1)/Anti-ICAM-1 Ab	ICAM-1	Anti-ICAM-1 Ab	100 ± 50	Willemsen *et al*. (1998)
Other protein/protein interactions				
Actin/actin in actin filaments			Not given	Moy *et al*. (1994a)
Cell adhesion proteoglycans	Proteoglycans	Proteoglycans	125	Dammer *et al*. (1995a)
The muscle proteins actin / myosin	Ultraavidin-coated fluorescent acrylamide nanobead with biotinylated myosin	Biotin adsorbed on tip	14.8 ± 4 and 24.7 ± 1.4	Nakajima *et al*. (1997)
Ab single-chain Fv (scFv) fragment / fluorescein	Ab single-chain Fv fragment (scFv) with an engineered C-terminal Cys residue	Fluorescein	50 ± 4	Ros *et al*. (1998)
Insulin/insulin	Insulin	Insulin	1300	Yip *et al*. (1998)
Citrate synthase/ *E. coli* chaperonin GroEL	GroEL	Citrate synthase	420 ± 100	Vinckier *et al*. (1998)
β-lactamase/ *E. coli* chaperonin GroEL	GroEL	β-lactamase	240 ± 70	Vinckier *et al*. (1998)
Recombinant P-selectin/P-selectin glycoprotein ligand-1(PSGL-1)	P-selectin	PSGL-1	~165	Fritz *et al*. (1998)
Osteopontin /αvβ3 integrin	αvβ3 integrin	Osteopontin	50 ± 2	Lehenkari *et al.* (1999)
Myelin basic protein/ lipid bilayers	Lipid bilayers	Myelin	~140	Mueller *et al*. (1999)

(Table 1) contd….

Molecular partners	on substrate	on AFM tip	Average forces (pN)	Reference
Other protein/protein interactions				
vascular endothelial (VE)-cadherins-Fc	VE-cadherins-Fc	VE-cadherins-Fc	15~150	Baumgartner *et al*. (2000)
Lactose/bovine heart(BHL)	BHL	Lactose	34 ± 6	Dettmann *et al*. (2000)
Lactose/lactose-binding immunoglobulin G(IgG)	Lactose	IgG	36 ± 4	Dettmann *et al*. (2000)
Lactose/*Viscum album*(VAA)	VAA	Lactose	47 ± 7	Dettmann *et al*. (2000)
Lactose/*Ricinus communis*(RCA)	Lactose	RCA	58 ± 9	Dettmann *et al*. (2000)
Asialofetuin(ASF)/BHL	*BHL*	*ASF*	37 ± 3	Dettmann *et al*. (2000)
ASF/VAA	VAA	ASF	43 ± 5	Dettmann *et al*. (2000)
ASF/IgG	ASF	IgG	45 ± 6	Dettmann *et al*. (2000)
ASF/RCA	ASF	RCA	65 ± 9	Dettmann *et al*. (2000)
Concanavalin A(Con A) receptor /Con A	Con A receptors on the surface of NIH3T3 fibroblast cells	Con A	86 ± 2.6	Chen and Moy (2000)
Human ocular mucins	Human ocular mucins	Human ocular mucins	100 ~ 1200	Berry *et al*. (2001)
Function-associated antigen-1 (LFA-1)/ intercellular adhesion molecule-1(ICAM-1)	ICAM-1	3A9 cell LFA-1	> 150	Zhang *et al*. (2002)
phospholipid bilayers / Recoverin	phospholipid bilayers	Recoverin	48 ± 5	Desmeules *et al*. (2002)
Receptor-associated protein (RAP) / its binding protein on living fibroblast cells	Binding protein on living fibroblast cells attached to surface.	Receptor-associated protein	120	Osada *et al*. (2003)
P-selectin/P-selectin glycoprotein ligand-1(PSGL-1)	P-selectin	PSGL-1	20	Marshall *et al*. (2003)
Cell adhesion proteoglycans	Proteoglycans	Proteoglycans	Not given	Popescu *et al*. (2003)
Ganglioside GM1/cholera toxin B-pentamer (ctB)	Ganglioside GM1	Cholera toxin B-pentamer (ctB)	Not given	Cai and Yang (2003)

section, we review AFM measurements of the interactions between surface-bound proteins and an AFM tip chemically modified with the protein-specific ligand.

3.2. Theory

The force necessary to rupture a bond may be calculated if the form of the potential is known. However, potentials have not been determined for complex protein interaction systems such as the streptavidin-biotin interaction which involve at least seven hydrogen bonds and a similar number of hydrophobic interactions. Unbinding forces for complex protein interactions have commonly been estimated by dividing experimentally determined bond energies (U) by a length (υ) that is thought to be representative of the range of the force, $F = -U/\gamma$ (Lee *et al*., 1994a). Using the ionic and van der Waals interactions as models, it appears that the effective rupture length, γ, increases with the range of the interaction potential or the inverse of the bond length. Given the nature of the bonding interactions in the protein-ligand system, we would expect the effective rupture length to be relatively short-ranged and similar to that of a van der Waals bond.

Bell (1978) has refined this simple model by taking into account the reversibility of specific interactions and the finite time over which the bond is ruptured. The external unbinding force F_{ub} applied to a reversible bond is related to the period, τ, over which the bond will rupture through the equation

$$F_{ub} = \frac{U - kT\ln(\tau/\tau_0)}{\ell} \qquad [2]$$

where U is the bond energy kT is the thermal energy, τ is the period over which the bond will rupture, τ_0 is the reciprocal of the nature frequency of oscillation, and ℓ is a characteristic length of bond (Evan *et al*., 1991).

3.3 Measurement

To determine the interaction forces between protein and protein-specific ligand with AFM, one of the binding pair partners is immobilized on a tip and the other on a substrate surface (or vice versa). During a force measurement cycle (see Fig. **5**), the tip is moved towards the surface at constant velocity until it is brought into contact with the sample (refer to Fig. **5**, position B). As the forward motion continues, the tip is pressed into the sample surface until a point of maximum load is reached (position C). The direction of motion is then reversed and the tip is withdrawn from the sample surface. A plot of cantilever deflection against distance moved by the fixed end of the cantilever is obtained as raw data. During the retraction portion of the force measurement, i.e., when the tip is withdrawn from the sample surface, the tip 'sticks' to the surface due to interactions between the tip and the sample. The magnitude of this adhesive force is calculated from the difference between the maximum cantilever deflection (position D) during the retraction portion of the curve and the point of zero cantilever deflection (position A). The cantilever deflection signal, measured in nAmp, is then converted to a deflection distance (nm), *d*, using the gradient of the retract trace in the contact region of the force curve (Allen, *et al*., 1996). This deflection distance, *d*, is converted to the force (nN) acting on the AFM probe using the cantilever spring constant, *k*, and Hooke's law ($F = -kd$). In this force curve, tip-surface adhesion is characterized as the maximum force needed to begin separation of the two pair partners after contact. Therefore, protein-ligand (or protein-protein) interactions between a tip coated with one half of a pair of the interacting species and a surface coated with the other half, can be identified by an increase in the magnitude of this force. The interpretation of the adhesion force, however, may be complicated by contributions from nonspecific interactions. Nonspecific interactions can arise from an improper spatial orientation of the protein and/or ligand that prohibits specific binding during the approach cycle and/or while in contact. Then the challenge is to identify those interactions that are specific, as opposed to nonspecific, in nature. This separation can be accomplished by conducting control experiments where, for example, the binding site on one of the partners in the protein-ligand or protein-protein pair is blocked. Because of the often random spatial orientation of the binding partners on the tip and surface, it is usually necessary to collect several hundred individual forces curves to determine a distribution of binding events.

Another essential requirement for the quantitative measurement of interaction forces is an accurate method for the calibration of the spring constant, *k*, of the AFM cantilever. Since the widely used commercially available silicon nitride cantilevers vary significantly in their spring constant (Cleveland *et al*., 1993), several methods for the calibration of AFM cantilevers have been proposed and are used in various laboratories (Cleveland *et al*., 1993; Hutter and Bechhoefer, 1994; Senden and Ducker, 1994). It has been shown that measured values for the spring constants differ significantly from the manufacturers' specifications (Cleveland *et al*., 1993). In light of the fact that the AFM is now used more frequently as a technique to measure interaction forces, it has become more critical that exact values are measured.

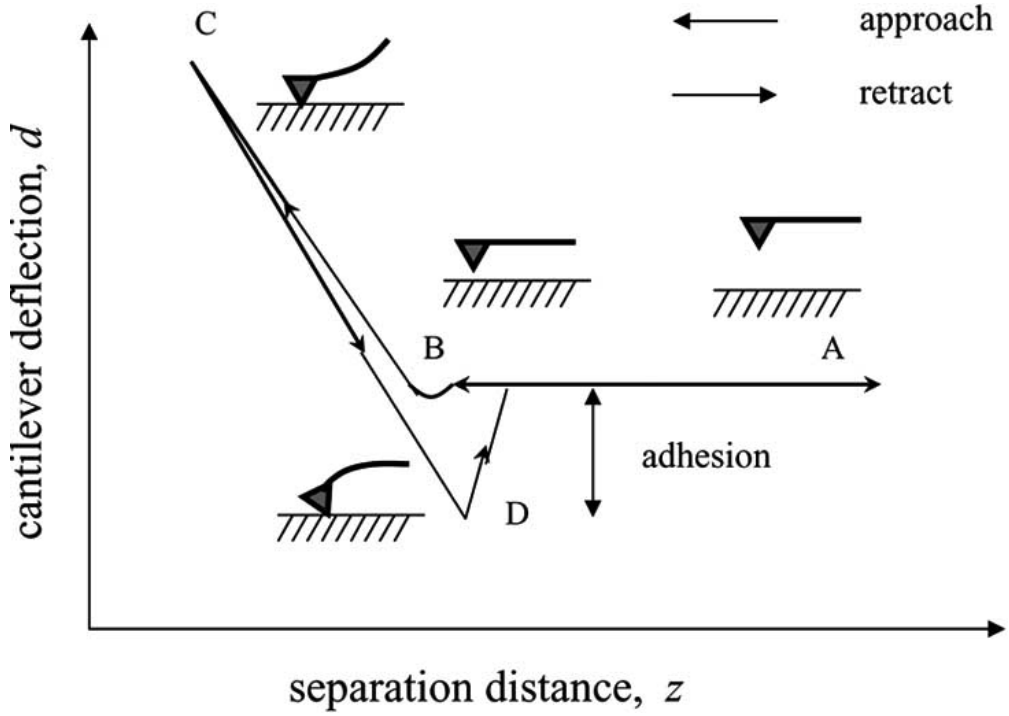

Fig. (5). A schematic diagram of a typical adhesion (unbinding force) measurement cycle. The relative position of the AFM tip to the sample surface is indicated and the direction of motion is indicated by the arrowheads. (A) zero cantilever deflection, (B) the tip is brought into contact with the sample surface, (C) the point of maximum load. (D) the point of maximum adhesive force. The cantilever deflection then returns to its original equilibrium position as the tip-sample separation is increased.

3.4. Examples

3.4.1. Avidin-Biotin Interactions

Avidin / Biotin Derivatives Interactions

Florin and co-workers (1994) were the first to measure biologically specific interaction forces of protein-ligand complexes. They measured the strength of the interaction between avidin on functionalized tips and biotin attached to a soft agarose bead (see Fig. **6A** for an illustration). Avidin, a 67 kDa protein from egg whites, is known for its high affinity for biotin, a cofactor in several metabolic reactions. Many of the initial investigations using AFM to probe protein interactions focused on the biotin-avidin system (Table **1**). This well-characterized pair was attractive as a starting point because of its high binding affinity ($K_d = 10^{-15}$ M). First, the sharp silicon nitride tips were incubated with biotinylated bovine serum albumin (BSA), a protein with biotin attached, which bound non-specifically and yet strongly to the tip. Afterwards, avidin was added to the biotin-labelled tips. Since there are multiple sites on the avidin for biotin binding, the unoccupied sites were then available for binding biotin attached to the agarose beads. After such a functionalized tip was in contact with the biotin-labelled substrate, the force curve showed distinct rupture steps (Fig. **6B**). In this work, soft biotinylated agarose beads were used as a surface to mimic biochemical affinity measurements. Thus, measured forces can be compared to thermodynamic data, obtained with those techniques. Another consequence of using the soft surfaces is that the contact area is significantly enlarged, resulting in multiple molecular bonds upon interaction of the tip with the bead. Although the use of multiple interaction sites may seem a complication, it actually facilitates the discrimination of quantized unbinding forces and increases the precision with which such a force can be measured (Willemsen *et al*., 2000). Because the rupture of the tip from the surface involved unbinding of many individual bonds, only the force of the final rupture was analyzed. The unbinding forces from more than 300 retraction experiments are summarized in a histogram, which reveals the quantization of unbinding forces in multiples of 160 ± 20 pN. This value was attributed to the interaction force of a single biotin-avidin binding pair.

3.4.2. Antibody-Antigen Interactions

Fluorescein / Anti-Fluorescein IgG Interactions

Promising results have been obtained from the biotin-(strept)avidin interaction model system (Lee *et al*., 1994a; Moy *et al*., 1994a, b). However, the biggest scientific challenges in this field, and potentially the most rewarding applications for the new technique, are related to the interactions between antibodies and antigens. Although the antibody-antigen interaction is of great practical and theoretical relevance, its direct study by force measurement is rendered more difficult by several factors. Both antibodies and antigens usually have complicated tertiary structures and need firm immobilization to the substrates. Their interactions depend on geometric factors, conformational state, and environment, and steric hindrance must be avoided (Davis and Padlan, 1990; Webster *et al*., 1994; Van Oss, 1994). The expected forces are in the piconewton range, and the antigen-binding sites of the antibodies are small compared with the antibody itself, so that nonspecific interactions must be considerated. Stuart and Hlady (1995) used a cantilever which was glued with a fluorescein-modified spherical silica bead to scan the surface-immobilized antifluorescein IgG molecules. They found that some intermittent discontinuities

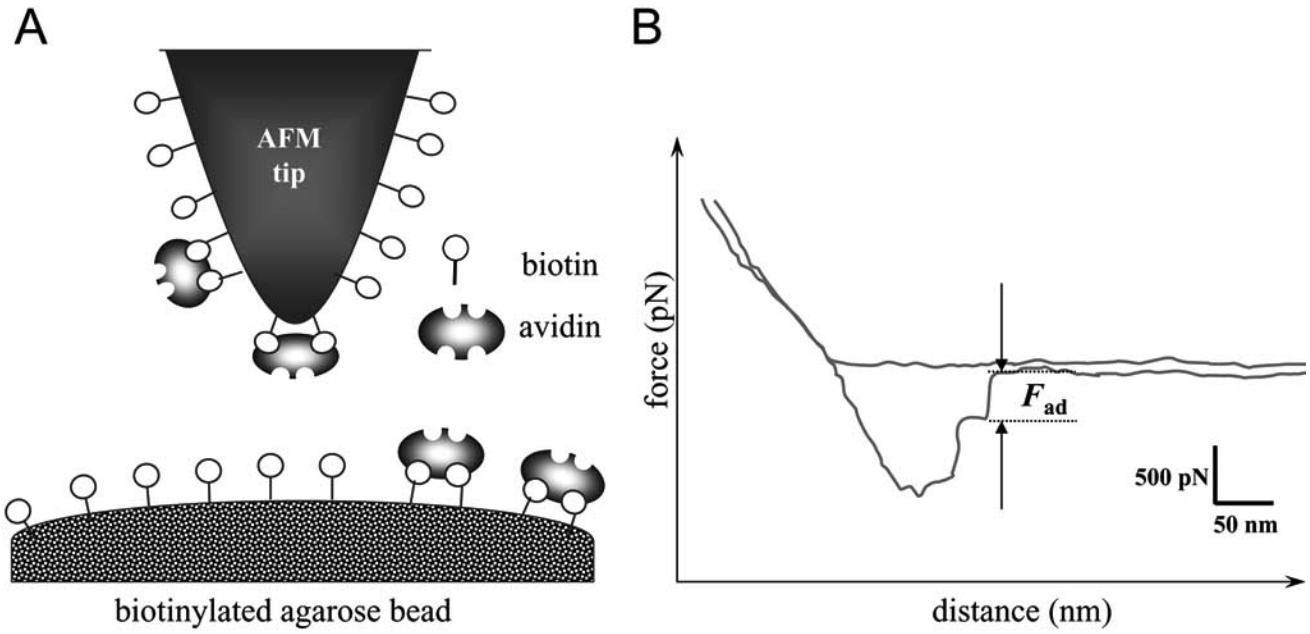

Fig. (6). (A) Schematics of the avidin-functionalized AFM tip and the biotinylated agarose bead. (B) Cantilever deflection curve on approach and retract of an avidin tip on a biotinylated agarose bead approximately 95% blocked with free avidin. F_{ad} is the measured adhesion (unbinding force) value.

in the force-displacement curves may be largely due to nonspecific discrete interactions between the antibody and the AFM probe. The strong lateral interactions which result in discontinuities observed in the adhesion curves are likely the result of localized adhesion due to the heterogeneous nature of proteins and the lack of molecular mobility.

Biotin / Anti-Biotin IgG Interactions

Dammer and co-workers (1996) followed a different approach using a self-assembled monolayer to functionalize tips and surfaces and measured the molecular interaction between BSA and polyclonal, biotin-directed IgG antibodies. The biotin was coupled *via* long (2.24 nm) spacer arms to BSA, and together with the BSA forms an artifical antigen. The advantage of this was found to be that the antigenic effect of the biotinylated BSA molecule containing 8-12 biotin moieties was less sensitive to conformational changes, steric hindrance, and orientation. The two components were then covalently immobilized on the AFM tip and on a flat gold surface *via* a ω-functionalized dialkyldisulfide cross-linker to quarantee stable and reproducible conditions. The chemisorption of the long-chain cross-linker in a self-assembly process provided a highly reactive monolayer surface for coupling primary amines under mild conditions. Furthermore, they used ultrasoft cantilevers for high force sensitivity and blocking molecules (BSA) to reduce nonspecific background. As a measure of the interaction strength, the size of the final jump from the surface peak in each curve was taken and averaged over a large number (> 3000) of different curves (> 1500). A mean binding force of 111.5 pN was determined. However, a histogram summarizing the retraction portion of the force curves suggested that the microcontact ruptured in quantized steps, each of ~0.06 nN. Though more speculative, an estimate of contact area argued that each rupture corresponded to the breakage of more than 1 but less than 10 interactions.

HSA / Anti-HSA IgG Interactions

Hinterdorfer and co-workers (1996) have created the largest mobilities of pairs by using the longer flexible spacer (6 nm) compared to 2.2 nm (Dammer *et al*., 1996) and by coupling human serum albumin (HSA) and polyclonal anti-HSA to the surface and the tip, respectively, *via* polyethylene glycol spacers. The tips were functionalized at such low anti-HSA density that, on average, only one single anti-HSA at the tip apex had access to an HSA on the surface. Moreover, HSA was coupled to the spacer at a packing density that statistically limited the interaction between the tip and sample to one interaction within the tip-sample microcontact. With this approach, the detected average unbinding force for 1:1 specific binding between HSA and anti-HSA was 244 ±22 pN. Analysis revealed that observed unbinding forces originate from the dissociation of individual Fab fragments from a HSA molecule. Also, the two Fab fragments of the antibody were found to bind independently and with equal probability. This investigation also demonstrated that the location of antigenic sites on the surface can be determined with a positional accuracy of 1.5 nm by scanning the tip laterally while collecting force scans. This approach was the first attempt to combine the ability of the AFM to detect specific protein interactions with the imaging capability that was already known for several years, and may be used to map binding sites and binding characteristics simultaneously.

Ferritin / Anti-Ferritin IgG Interactions

Allen and co-workers (1997) also investigated the adhesive forces between ferritin-functionalized AFM probes and anti-ferritin antibody-coated silicon substrates. Polystyrene microtiter well surfaces functionalized with anti-ferritin antibody provide the analyte capture component of an immunoassay, which can be employed to detect serum ferritin levels. Analysis of the force distribution data also suggested a quantization of the forces, with a period of 49 ±10 pN. However, even though such an immunoassay system has been developed, little is known about how the ferritin molecules are bound to the antibodies. The polyepitopic nature of the ferritin molecule allows the binding of more than one antibody molecule to each molecule of ferritin, thereby increasing the chance of observing multiple binding events in force measurements. Therefore, in instances where structural or thermodynamic data may be limited, a direct measure of the strength of the antigen-antibody bond by AFM can give glimpses into the binding process.

3.4.3. Other Protein/Protein Interactions

Chaperonin GroEL/ Citrase Synthase Interactions

Vinckier and co-worker (1998) investigated the structure of the *Escherichia.coli* chaperonin GroEL by tapping-mode AFM under liquid and measured the interaction forces between the *E. coli* chaperonin protein GroEL and two different substrate proteins. High-resolution images were obtained, which show the up-right position of GroEL adsorbed on mica with the substrate-binding site on top. Because of the upright orientation of GroEL on mica, AFM was used to quantitatively measure the interaction force between GroEL and the substrate proteins, (Gly-Ala) citrate synthase (770 ± 190 pN) and (Cys-Ala) β-lactamase (350 ± 100 pN), by covalently immobilizing them on the surface of the tip. The results showed that the interaction force decreased in the presence of ATP, which resulted in conformational changes in the GroEL apical domains, and that the force was smaller for native proteins than for the fully denatured ones. Similarly, it was found that denatured proteins gave rise to a higher interaction force than the native proteins. This finding may prove of value in furthering insight into the denaturation process.

P-Selectin / P-Selectin Glycoprotein Ligand-1 (PSGL-1) Interactions

Leukocyte rolling is a good example of how the mechanical properties of single molecules determine the characteristics of cell-cell adhesion. P-selectin, located on the endothelial cell wall, supports leukocyte rolling under hydrodynamic flow *via* interactions with its glycoprotein counter ligand P-selectin glycoprotein ligand-1 (PSGL-1) expressed on microvilli of the leukocyte surface (McEver *et al*., 1995). P-selectin-PSGL-1 binding involves interacting sites that are located close to the amino-terminal portion of each molecule and furthest away from the cellular membrane (McEver *et al*., 1995). Under the hydrodynamic drag forces of blood flow, rolling is mediated by the interaction between

selectins and their ligands across the leukocyte and endothelial cell surfaces (Fig. **7**). Fritz and co-workers (1998) used AFM to perform experiments on single complexes of P-selectin and P-selectin glycoprotein ligand-1 and to determine the intrinsic molecular properties of this dynamic adhesion process. By modeling intermolecular and intramolecular forces as well as the adhesion probability in AFM experiments they obtained information on unbinding forces of the P-selectin-P-selectin glycoprotein ligand-1 interaction. The complexes were able to withstand forces up to 165 pN and showed a chain-like elasticity with a molecular spring constant of 5.3 pN nm^{-1} and a persistence length of 0.35 nm. Unbinding force and lifetime of the complexes were not constant, but directly depended on the applied force per unit time, which is a product of the intrinsic molecular elasticity and the external pulling velocity. The high strength of binding combined with force-dependent rate constants and high molecular elasticity were tailored to support physiological leukocyte rolling (Fig. **7**).

Recoverin/Lipid Bilayers Interactions

Recoverin is a 23-kDa calcium-binding protein originally purified from retinal rod outer segments of vertebrates (Dizhoor *et al*., 1991). This protein is a member of the EF-hand superfamily, which contains proteins that bind Ca^{2+} *via* the EF-hand motif, a helix-loop-helix of 12 residues arranged to coordinate Ca^{2+} with pentagonal bipyramidal symmetry (Braunewell and Gundelfinger, 1999). Ca^{2+} binding by recoverin induces the extrusion of its myristoyl group to the solvent, which leads to its translocation from cytosol to rod disk membranes. Force spectroscopy, based on AFM technology, was used to determine the extent of membrane binding of recoverin in the absence and presence of calcium, and to quantify this force of binding (Fig. **8**) (Desmeules *et al*., 2002). An adhesion force of 48 ± 5 pN was measured between recoverin and supported phospholipid bilayers in the presence of Ca^{2+}. However, no binding was observed in the absence of Ca^{2+}. Experiments with non-myristoylated recoverin confirmed these observations.

3.4.4. Individual Protein Interactions

As shown in Table **1**, initially emphasis was placed on study of the avidin-biotin interaction, which was the primary model exploited by several laboratories. In these studies, however, the number of molecules involved in the measured force was not determined directly, moreover binding processes were not observed at a single molecular level. Although the method of Florin and co-worker (1994) is very useful in determining the unbinding forces of discrete bonds, they predominantly observed the parallel breakage of multiple bonds. This is a consequence of their tip-sample configuration, which does not allow the repetitive addressing of the same individual molecules. To really measure interactions between single molecules, very strict conditions need to be fulfilled. The density of molecules distributed both on tip and surface should be sufficiently low to allow the formation of single molecular interactions. In AFM experiments, this implies that the surface coverage of active molecules on the

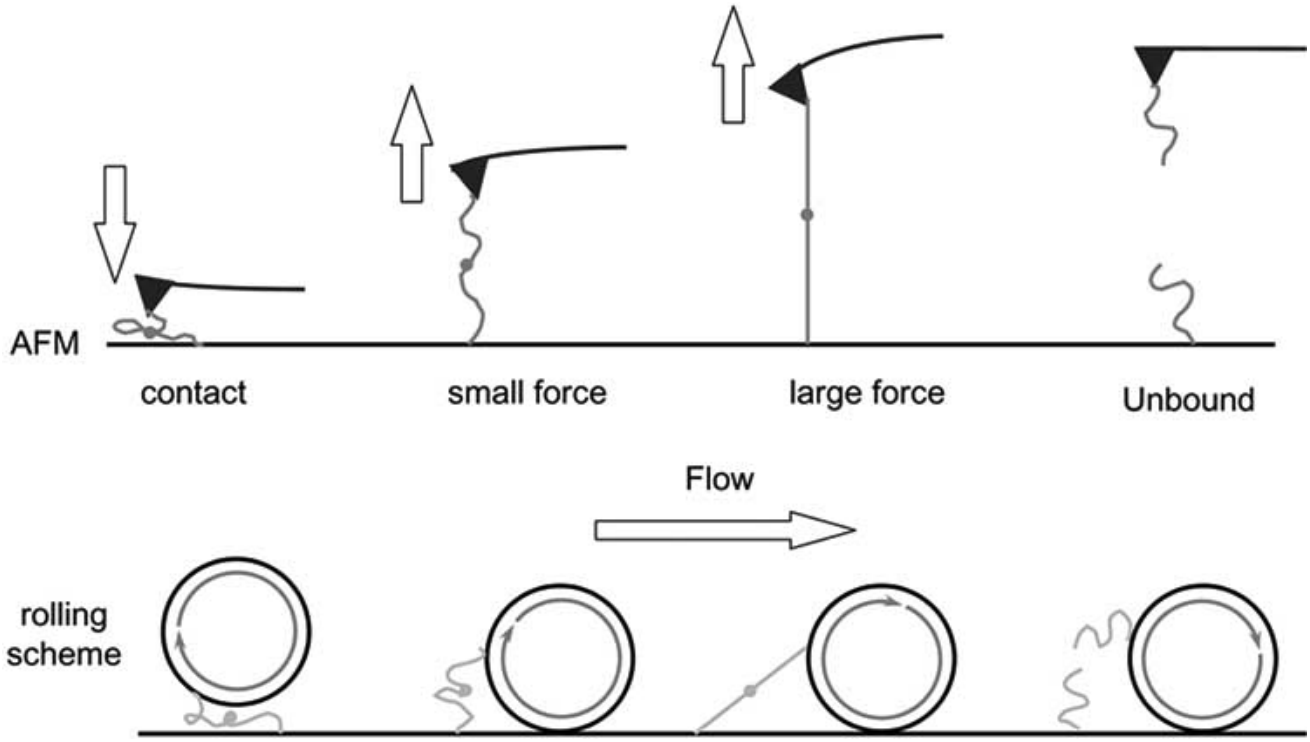

Fig. (7). Schematic representation of selectin-ligand interaction during leukocyte rolling on venular endothelium in AFM experiments. The approach and retraction of the AFM tip simulates the physiological rolling process. After binding, the force on the complex increases continuously with increasing tip-surface distance. After rupture, the chain-like molecules shrink to their equilibrium length, and their binding sites, both located close to the amino-terminal ends of the molecules, are separated.

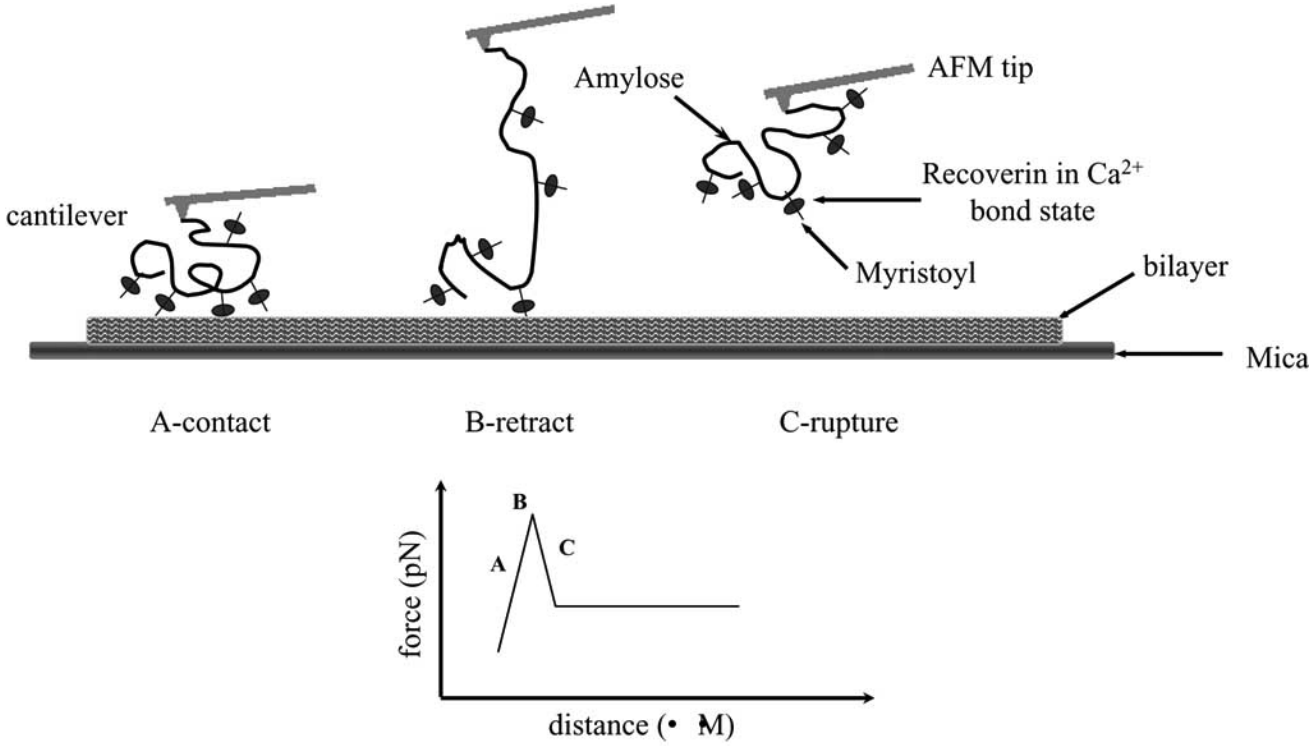

Fig. (8). Schematic diagram of the experimental setup. Myristoylated recoverin was covalently tethered *via* a carboxymethylated amylose spacer to the AFM tip. In the presence of Ca^{2+}, adhesion between the myristoylated recoverin tip and the bilayer was observed. This adhesion causes an extra force signal during tip retraction until the rupture between recoverin and the bilayer occurs. (*A*) The tip is brought into contact with the bilayer. (*B*) The tip is retracted from the bilayer. (*C*) The bridge between recoverin and the bilayer is ruptured.

tip or surface should be chosen sufficiently low to allow for single molecular interactions. To verify distribution of molecules on the tip, investigators have modified flat substrates, consisting of the same material as the tip, in the same batch. Subsequently, molecular distribution is determined with conventional surface techniques, such as fluorescence microscopy (Nakajima *et al*., 1997) or tapping mode AFM (Willemsen *et al*., 1998).

Actin-Heavy Meromyosin /Actin Interactions

Nakajima and co-workers (1997) were the first to measure the protein-protein interaction force with AFM at a single molecule level. They integrated the AFM and an epifluorescence microscope to develop a method to capture a single molecule of heavy meromyosin at an AFM probe tip and observed the interaction force between the captured meromyosin and actin fixed on the surface. A strategy for linking a single molecule of meromyosin to a cantilever tip is sketched in Fig. **9**. The unbinding event and the binding event were observed from which knowledge of the inter-protein force field was obtained at a single molecular level. The unbinding force of a single head-actin pair was around 14.8 pN, an order of magnitude smaller than other inter-protein forces (Dammer *et al*., 1995b; Hinterdorfer *et al*., 1996), while the effective rupture length (1.7~2.5 nm) was long compared to other measured values, 0.23 nm for antigen-antibody (Hinterdorfer *et al*., 1996), 0.15~0.3 nm for streptavidin-biotin (Lee *et al*., 1994a) and 0.05~0.3 nm for actin-α-actinin (Miyata *et al*., 1996).

3.4.5. Multivalent Protein Interactions

Biological recognition or adhesion is not typically mediated by single, high-affinity interactions, but by many weak contacts. The advantage of the latter is that weak interactions allow for formation of dynamic contacts, the plasticity in adhesive junctions, and cell motility (Fritz *et al*., 1998). Because low-affinity bonds are believed to exhibit short lifetimes and low rupture forces, adhesion requires multiple such interactions. Many cell adhesion molecules contain large, multidomain extracellular segments, and some exhibit multiple contacts with their corresponding ligands (Chothia and Jones, 1997). While multiple interactions may contribute to binding, their implications for protein-mediated adhesion have not been explored.

Cell Adhesion Proteoglycans Interactions

To investigate how the rupture of multiple contacts might differ from single-bond failure, Dammer and coworkers (1995a) measure the binding forces intrinsic to adhesion molecules to assess their contribution to the maintenance of the anatomical integrity of multicellular organisms. AFM was used to measure the binding strength between cell adhesion proteoglycans (AP) from marine sponge. The shape of the approach-and-retract cycles shows that stringlike structures were responsible for AP-AP interactions (Fig. **10**). These strings are likely to be the AP arms which have been shown to mediate polyvalent AP-AP binding (Misevic *et al*., 1987). During each approach-and-retract cycle, multiple non-covalent bonds between arms attached to the sensor tip

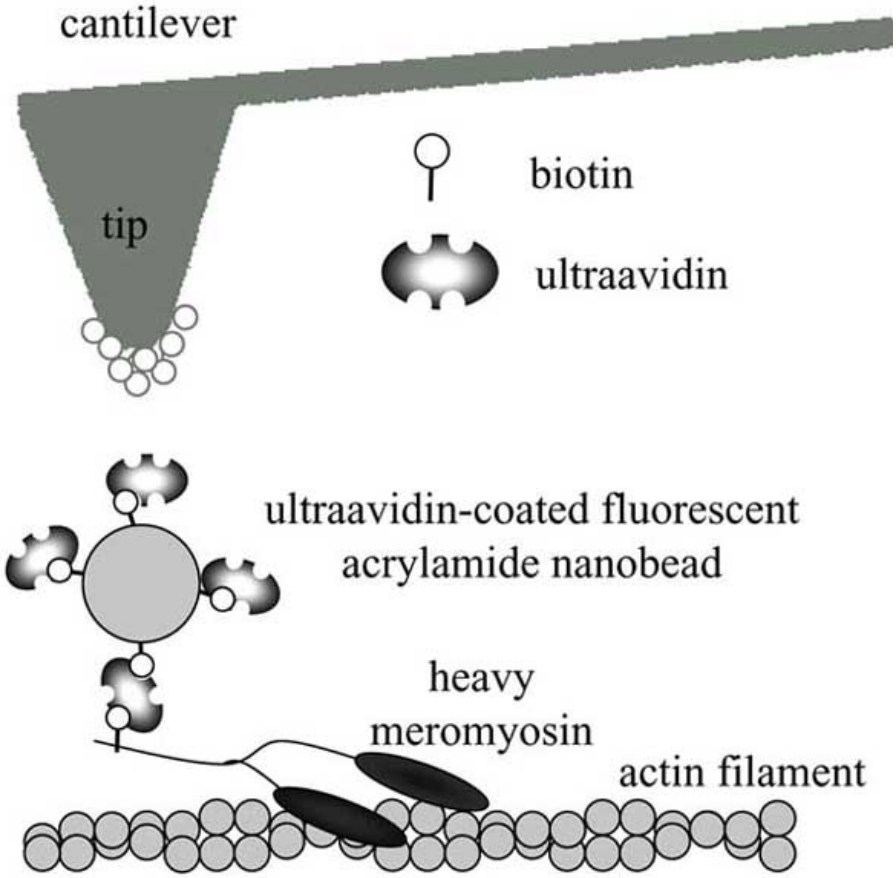

Fig. (9). Strategy to link a single molecule of heavy meromyosin to an AFM tip. This strategy is based on the strong affinity of biotin for avidin. The distal end of the tail part of heavy-meromyosin was specifically modified with biotincadaverine and ultraavidin was used instead since avidin has a tendency to bind to proteins non-specifically.

and arms connected to the substrate were formed and broken. Because the radius of curvature of a typical functionalized AFM tip used was about 50 nm and the AP backbone ring was approximately 200 nm in diameter, only a single AP molecule from the tip could participate in the measured interaction with the densly AP-covered surface. The observation that approach-and-retract curves often exhibited multiple jump-off steps (Fig. **10**) indicates that binding was polyvalent. Each step of 40 ± 15 pN corresponded to the unbinding of a pair of AP arms, with deviation caused by a varying degree of mutual overlap. The maximal measured adhesion force of 400 pN and the average force of 125 pN were thus interpreted as the binding between 10 and 3 pairs of AP arms.

3.4.6. Stretching of Multi-Domain Proteins

The three-dimensional structure of proteins is stabilized by many different and competing interactions. Their stability or resistance to unfolding are typically investigated by chemical or thermal denaturation (Politou *et al*., 1995). Many proteins, however, are designed to withstand forces rather than heat or a harsh change in their chemical environment; their role is to maintain a certain structure against an external load. Because the energy landscape of protein folding (Frauenfelder *et al*., 1991) is yet unknown, mechanical properties or unfolding forces of proteins cannot be derived by thermal or structural analysis and must be measured. AFM is capable of measuring the forces required to unfold protein domains with piconewton (pN) sensitivity and the length changes with Angstrom resolution. In this configuration, a single protein is suspended between an AFM tip and a substrate. In a typical experiment (see Fig. **11**), the tip is brought into contact with a layer of protein attached to the substrate, then the piezoelectric positioner retracts. When a portion of a single protein molecule is picked up at random by the tip through adsorption, the retraction of the positioner stretches the suspended segment of the protein. The first source of resistance to extension of the protein are entropic forces. As the distance between substrate and cantilever increases, the protein elongates and the reduction of its entropy generates a restoring force that bends the cantilever. When a domain unfolds, the contour length of the protein increases returning the force on the cantilever to near zero. We summarize the available literature about the stretching of multi-domain proteins in Table **2**.

Stretching of Titin Immunoglobulin Domains

The muscle protein titin is responsible for the passive elasticity of muscle fibers and consists of a sequence of more than 200 modules, so called immunoglobulin domains (Ig domains), each consisting of about 90 amino acids, which form a beta barrel. Rief and co-workers (1997) have used AFM to study unfolding forces of single titin-Ig domains. Individual titin molecules were repeatedly stretched, and the

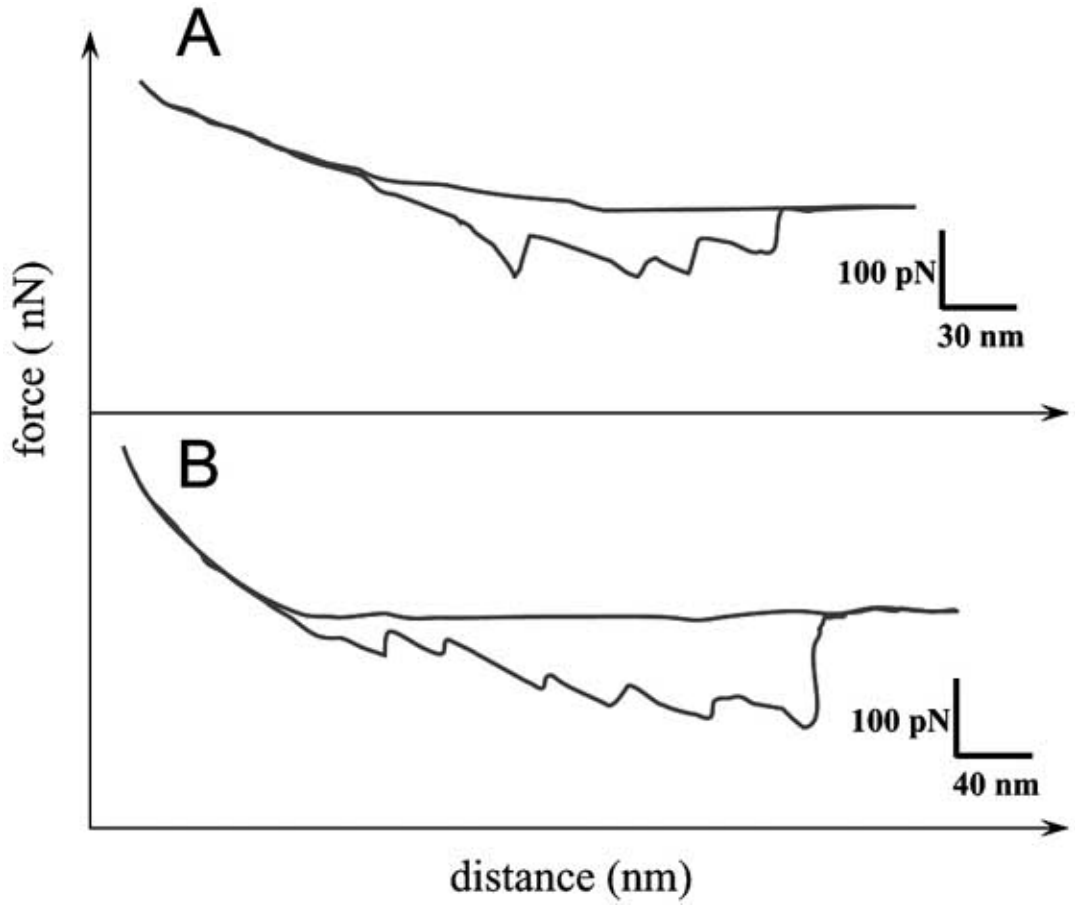

Fig. (10). Two typical AFM approach-and-retract cycles for cell adhesion proteoglycan (AP)-AP interactions. Multiple jump-offs in both (A) and (B) indicate polyvalent binding with an average adhesive force of 40 ± 15 pN per release.

applied force was recorded as a function of the elongation. At large extensions, the restoring force exhibited a sawtooth like pattern, with a periodicity that varied between 25 and 28 nm. This periodicity is in good agreement with the expected length required to unfold individual Ig domains. To test this hypothesis, recombinant Ig4 and Ig8 fragments were constructed. Eight peaks were observed in the elongation plots for Ig8 and four with Ig4. The forces required to unfold individual domains ranged from 150 to 300 pN and depended on the pulling speed. This quantization is further evidence for the sequential unfolding of individual Ig domains, demonstrating the ability of AFM to probe unfolding force at the level of single tertiary structures of proteins.

4. FORCE MAPPING OF PROTEINS

In a new method called force mapping, force-distance curves are recorded at each sample point of an image. An increasingly accepted way of displaying such data is as force-volume plots. Heinz and Hoh (1999a) have reported an excellent account of the acquisition of force-volume data and also reviewed the general interpretation of such data for mapping biological surfaces. The force volume plot consists of a topographical image of an area of the biological sample together with an array of force-distance curves recorded over the same area. The data can be displayed as slices of the volume plot showing force at constant height, slices corresponding to constant force images, or as individual force-distance curves. Data are recorded for both approach and retraction from the surface. In studies of protein systems, the force-distance data can contain information on sample adhesion (as shown in section 4.1), elasticity (section 4.2), viscosity (section 4.2), surface charge density (section 4.3), or other factors modifying the force-distance curve such as specific intermolecular binding. Thus the force volume data can be used to generate different types of force maps which can be utilized to generate different types of contrast for comparison with normal topography images (Morris *et al*., 1999).

4.1. Adhesion Mapping

4.1.1. Introduction

Adhesion (unbinding force) mapping can be used to map tip-sample binding and hence, if ligand-functionalized tips are used, specific structures and recognition events can be identified on protein surfaces (or vice versa). Adhesion maps can be generated by selecting the most negative force on the retraction curve and plotting isoforce maps (which is based on a surface of equal force collected over (or below) the sample surface) as a function of position on the surface. This approach overcomes one of the difficulties with AFM imaging which is identification of surface features.

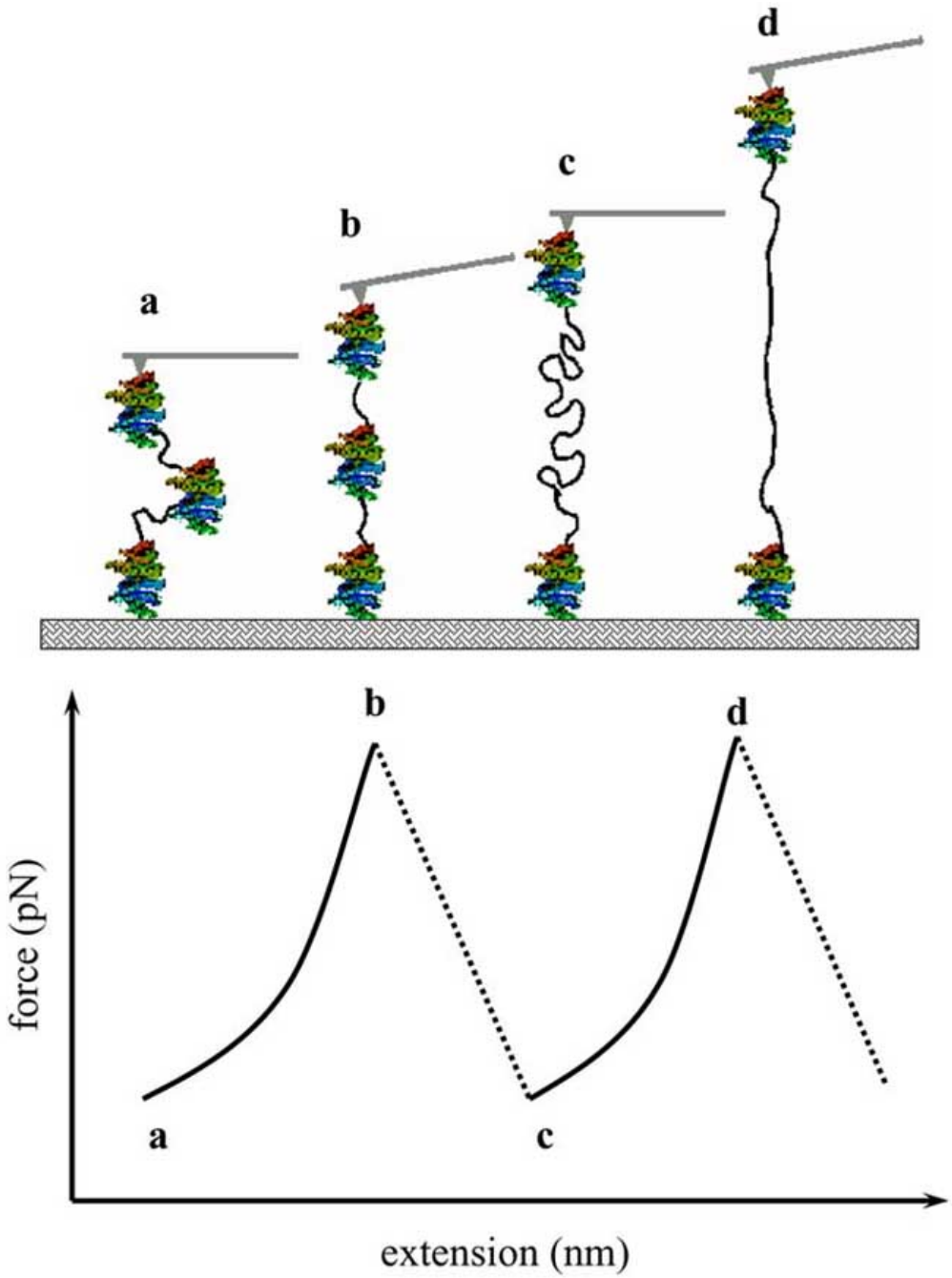

Fig. (11). Schematic showing the structural transitions in multidomain proteins which give rise to the multi-peak force curves, as those represented in Fig. 4E. As the distance between substrate and cantilever increases (from states a to b) the protein elongates and the reduction of its entropy generates a restoring force that bends the cantilever. When a domain unfolds (state c) the contour length of the protein increases, returning the force on the cantilever to near zero. Further extension again results in force on the cantilever (state d).

4.1.2. Measurement

Adhesion maps are typically produced by taking the most negative force detected during the retraction curve as the value for adhesion and plotting that value against the *x-y* position of each curve. Several types of spatially resolved adhesion map have been produced. There are two basic approaches to producing the spatial distribution of forces within a volume using an AFM. The first is to collect an array of force curves over the surface and assemble these into a force volume representation. The second is to reconstruct the same force volume data by collecting a series of isoforce images, at increasing or decreasing forces, across the x-y plane and assembling these. However, this is not possible in practice with current instruments. For simultaneous measurements of topography and adhesion, the force-distance mode is used.

4.1.3. Examples

BSA-biotin / Streptavidin Interactions

The feasibility of this approach to adhesion mapping was shown for the first time by Ludwig and co-workers (1997) by using biotinylated tips to map distributions of streptavidin on a patterned surface. The method was termed affinity imaging and was used to compare topographical and adhesion maps of the protein sample. In this mode, topography and adhesion force were extracted online from local force scans. The adhesion histogram obtained showed that the adhesion had a broad distribution and was centered at about 1000 pN. Taking into account that the unbinding force of individual molecular pairs is 250 pN, this adhesion seemed to be caused by several molecular pairs in parallel. To confirm that the measured adhesion image was due to specific molecular recognition, the protein sample was blocked by adding an excess of free biotin. Under these conditions virtually no contrast was measured in the affinity image, whereas the topography contrast did not change.

Intercellular Adhesion Molecule-1 (ICAM-1) / Anti-ICAM-1 Interactions

Willemsen and co-workers (1998) simultaneously measured the topography and adhesion images with a resolution of 20 and 5 nm, respectively. They imaged a submonolayer of intercellular adhesion molecule-1 (ICAM-1) antigen in adhesion mode and demonstrated that the resolution of the topographical image in adhesion mode was only limited by tip convolution and thus comparable to tapping mode images. The high-resolution height image showed individual ICAM-1 molecules that corresponded very well to bright adhesion pixes, thus indicating spacially resolved specific protein interaction. The topographical image taken at a high surface concentration also showed the contrast between clusters of ICAM-1 and the mica substrate, while the adhesion image showed many bright pixels on top of clusters of molecules (Fig. **12**), which gave evidence of the molecular interaction process between individual ICAM-1 antigens and antibodies . Also, all evidences showed that the force peaks in the adhesion image were mainly caused by single molecular interactions. Therefore, by comparing the high-resolution height image with the adhesion image, it was possible to show that specific molecular recognition was highly correlated with topography. The stability of the improved microscopy enabled imaging with forces as low as 100 pN and ultrafast scan speed of 22 force curves per second. The analysis of force curves also showed that reproducible unbinding events on subsequent scan lines could be measured.

4.2. Elastic and Viscous Force Mapping

4.2.1 Introduction

The elastic properties of protein materials can be determined accurately and spatially well with AFM force curves by relating the applied force to the depth of indentation as the tip is pushed against the sample. The indentation may be elastic, i.e., reversible; dynamic, i.e., viscous; or plastic, i.e., irreversible in nature; or a combination of the three. When the stress, i.e., the deformation force, and the strain, i.e., the amount of deformation, are linearly related, the deformation of the protein material is elastic, and the material will regain its original form upon relaxation. The depth of indentation can be used to measure local elasticity in terms of Young's (elastic) modulus (Fritzsche and Henderson, 1997; Vinckier and Semenza, 1998; Zelatanova *et al*., 2000) (Fig. **13**). Although this is not an interaction force per se, we include it because it is a widely used application of AFM and because the elasticity of biological sample is often coinvolved with real interaction forces.

In addition, the behavior of soft protein samples shows another type of deviation from that of a hard surface. Whereas the lift-off occurs quickly on hard surfaces, it may be considerably slowed down in the case of soft protein samples (Fig. **14**). The lift-off speed may be used to estimate the viscosity of the protein sample (Radmacher *et al*., 1994).

4.2.2. Theory

For quantifying the elastic properties of a protein sample, a range of data from the force curve to be analyzed and an appropriate model for analysis must be chosen. The most simple model comes from continuum mechanics (Hertz, 1882), which was extended by Sneddon (1965). For an introduction in continuum mechanics, one may visit the work of Fung (1993) and Treloar (1975). Using AFM, elasticity measurements are performed by pushing a tip onto the surface of the sample of interest and monitoring force-versus-distance curves. This results in a deformation which is the sum of the deformation of the tip and the deformation of the investigated sample (indentation) under the tip. Although AFM is measured on a microscopic scale, the classical theory is still usable because the tip indents 100 or more atoms of the surface (Vinckier and Semenza, 1998).

The Hertz model describes the elastic indentation of an infinitely extended sample (effectively filling out a half-space) by an indenter of simple shape. Two shapes of indenter often used in AFM are conical or parabolic tips:

For a conical tip with a semivertical (open) angle α, the total force F_{cone} as a function of the indentation Δz is described by:

$$F_{\text{cone}} = \frac{2\tan(\alpha)E}{(1-\nu^2)\pi}\,\Delta z^2 \qquad [3]$$

The force $F_{\text{paraboloid}}$ as a function of the identation for a parabolic tip with a radius of curvature R at the apex is:

$$F_{\text{paraboloid}} = \frac{4\sqrt{R}}{3(1-\nu^2)}\,E\Delta z^{3/2} \qquad [4]$$

Here, F_{cone} is the force needed to indent an elastic protein sample with a conical tip, whereas $F_{\text{paraboloid}}$ is the force needed to indent the protein sample with a parabolic tip. A spherical tip with a radius R also leads to the same formula as Eq. [4], as long as the contact radius $r \leq R$. The indentation is denoted by Δz , whereas E is the elastic or Young's modulus, ν is the Poisson ratio, α is the half-opening angle of the cone, and R is either radius of curvature of the parabolic tip or the radius of the spherical tip, respectively. The above description assumed deformations arising from perfectly flat elastic substrates; however, some of the contributions such as (1) plastic deformations, (2) the surface energy, and (3) the local shape of a rough surface can

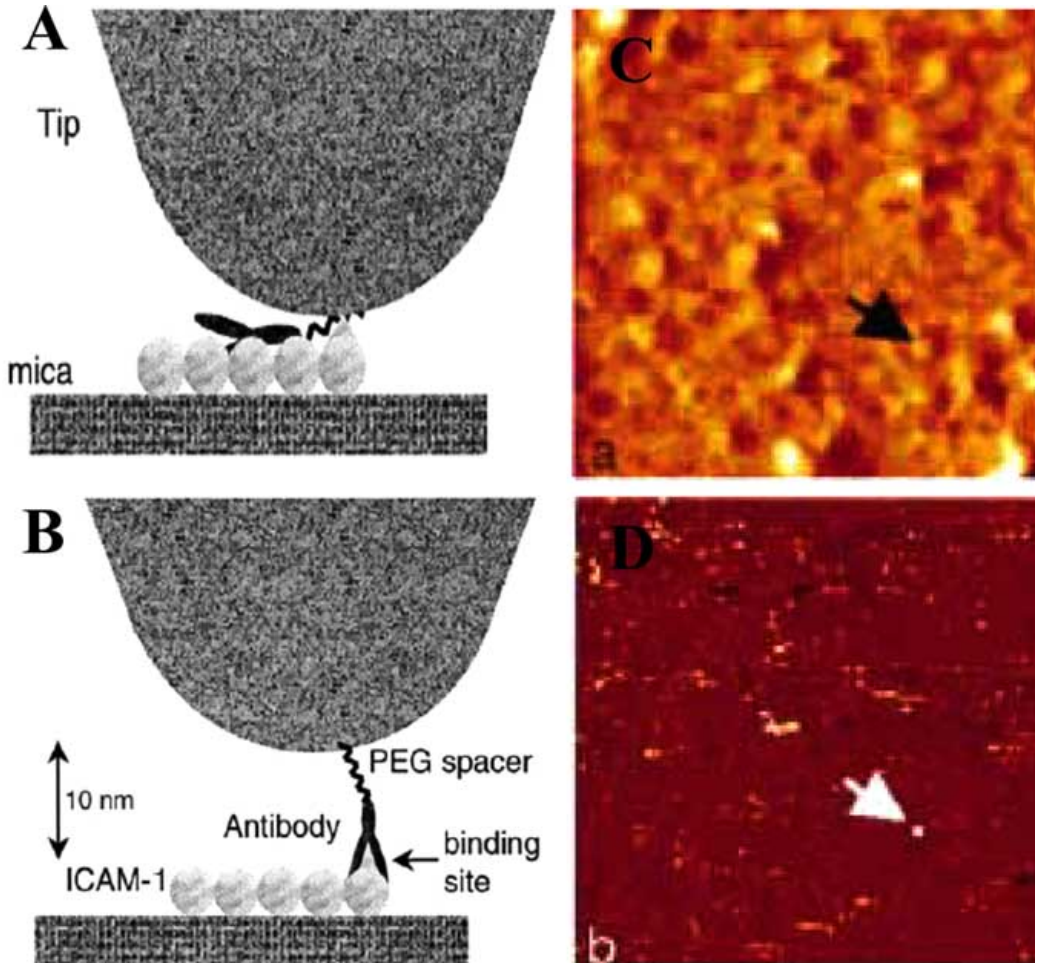

Fig. (12). Schematic representation of the geometrical situation at height (A) and adhesion (B) measurement, which explains the tip and spacer convolution, respectively. Simultaneously measured height (C) and adhesion (D) images of ICAM-1, adsorbed to mica, recorded in PBS with a functionalized tip with anti-ICAM-1 antibodies. Image size 400 x 400 nm, z-range 0-5 nm. Reprinted with permission from reference (Willemsen *et al*., 1998). Copyright 1998 the Biophysical Society.

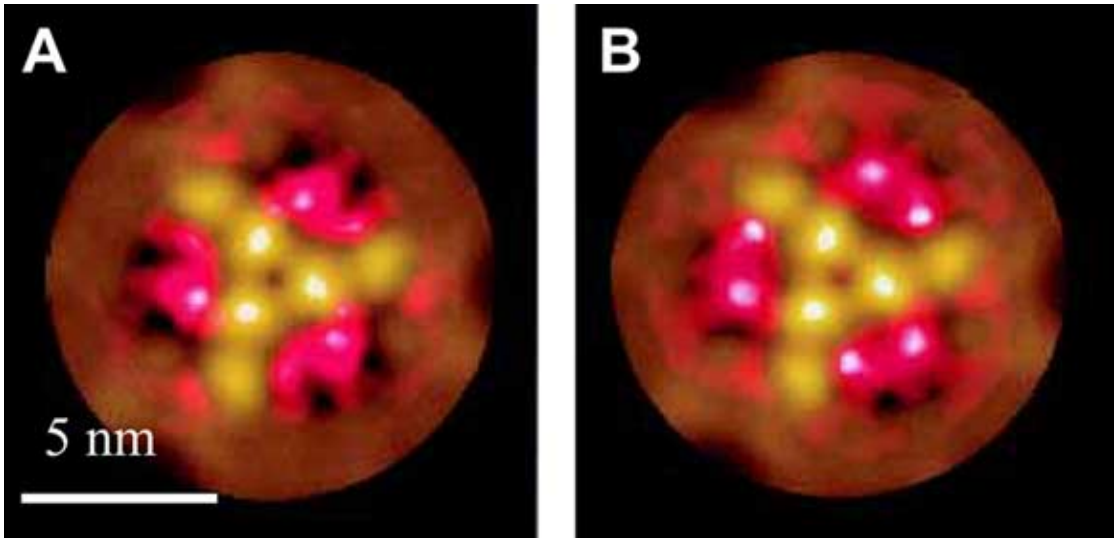

Fig. (17). Electrostatic potential mapping of the OmpF porin channel. The superimposition of the electrostatic potential (red to white) and of the AFM topograph (brown yellow) was shown. The electrostatic potentials represent difference maps calculated from topographs recorded at different electrostatic contributions, 300 and 50 mM KCl (A), and 300 and 100 mM KCl (B). Reprinted with permission from reference (Philippsen *et al*., 2002). Copyright 2002 the Biophysical Society.

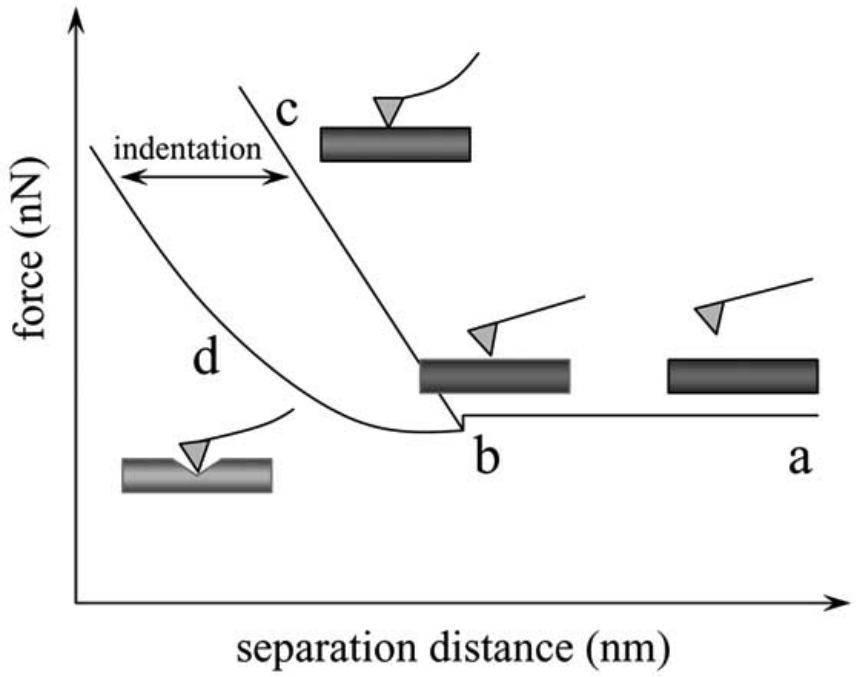

Fig. (13). Schematic representation of typical approach force-versus-distance curves on a hard (a-b-c) and a soft protein sample (a-b-d). The picture (a) shows the situation with no contact between tips and sample and in (c) a hard sample results in a deflection of the cantilever. Picture (d) shows the deformation of the protein sample by the tip which results in deviation from the linear relationship between the force and the distance. The difference in deflection between the two curves is a measure of indentation.

considerably influence the measured Young's modulus (Vinckier and Semenza, 1998).

4.2.3. Measurement

Local elastic properties of proteins can be determined by AFM. In principle, one can maintain the AFM tip at each image point for a fraction of a second with a fixed sample-tip distance while recording the deflection of the cantilever (Putman *et al*., 1994). With this approach the image, also three dimensional, contains dynamic information that reflects the rearrangement of the protein surface under prolonged stress. Another method is to acquire a force curve in a given range at each image point, resulting in a three-dimensional image. Then a series of images at different probe forces can be generated where the changes in height on the surface could reflect the elastic property of the protein sample. Such an approach has been demonstrated by Radmacher *et al*., (1994). A major challenge for this type of application is the interpretation of the resulting images. At present, it is not clear what kind of information is contained in these images and how to test various possibilities. However, because of the difficulty of achieving very small forces and stable imaging at high resolution, the application at the molecular scale has not been reliable, except for the case of cryogenic atomic force microscopy (cryo-AFM). Since the elastic response of a protein macromolecule is probably nonlinear, the value at a large probe force may not have any physiological meaning, because these biomolecules are not subject to such a large deformation *in vivo* (Shao *et al*., 1996).

4.2.4. Examples

Recent studies have shown that elastic properties of cells can be detected with the AFM (Hoh and Schoenenberger, 1994). Quantitative analysis of the elastic properties can be obtained with the AFM by taking force curves. AFM force curves have also been used to examine the elastic properties of a wide range of protein structures (Vinckier and Semenza, 1998; Heinz and Hoh, 1999a). The Young's modulus of thin films of lysozyme was measured to be 500 ± 200 MPa (Radmacher *et al*., 1994), that of microtubules to be 3 MPa (Vinckier *et al*., 1996), and that of gelatin to be 20 kPa (Radmacher *et al*., 1995; Domke and Radmacher, 1998). In addition, imaging of elastic properties with the AFM is possible using force modulation (Radmacher *et al*., 1993; Baselt, 1994), which has been applied to platelets (Radmacher *et al*., 1992; Radmacher *et al*., 1996) and magnetotactic bacteria (Fritz *et al*., 1994).

Elastic Force Map of Thin Gelatin Films

Domke and Radmacher (1998) have investigated the elastic properties of thin gelatin films with the AFM. They tuned the degree of swelling and thus the softness of the gelatin by immersing it in mixtures of propanol and water. The influence of the film thickness on the apparent Young's (elastic) modulus of gelatin was investigated (Fig. **15**). The Young's modulus of the prepared samples was between 1 MP and 20 kPa depending on the degree of swelling. The elasticity was calculated by analyzing the recorded force curves with the help of the Hertz model. They showed that the calculated Young's modulus is dependent on the local film thickness and the applied loading force of the AFM tip. If the gelatin film is >1 μm and the Young's modulus is >20 kPa, the Hertz model matches the data over a wide range of loading forces. However, for thinner films, there is a disagreement between the model and the experimental data. With these ultrathin films, the hard underlying substrate is

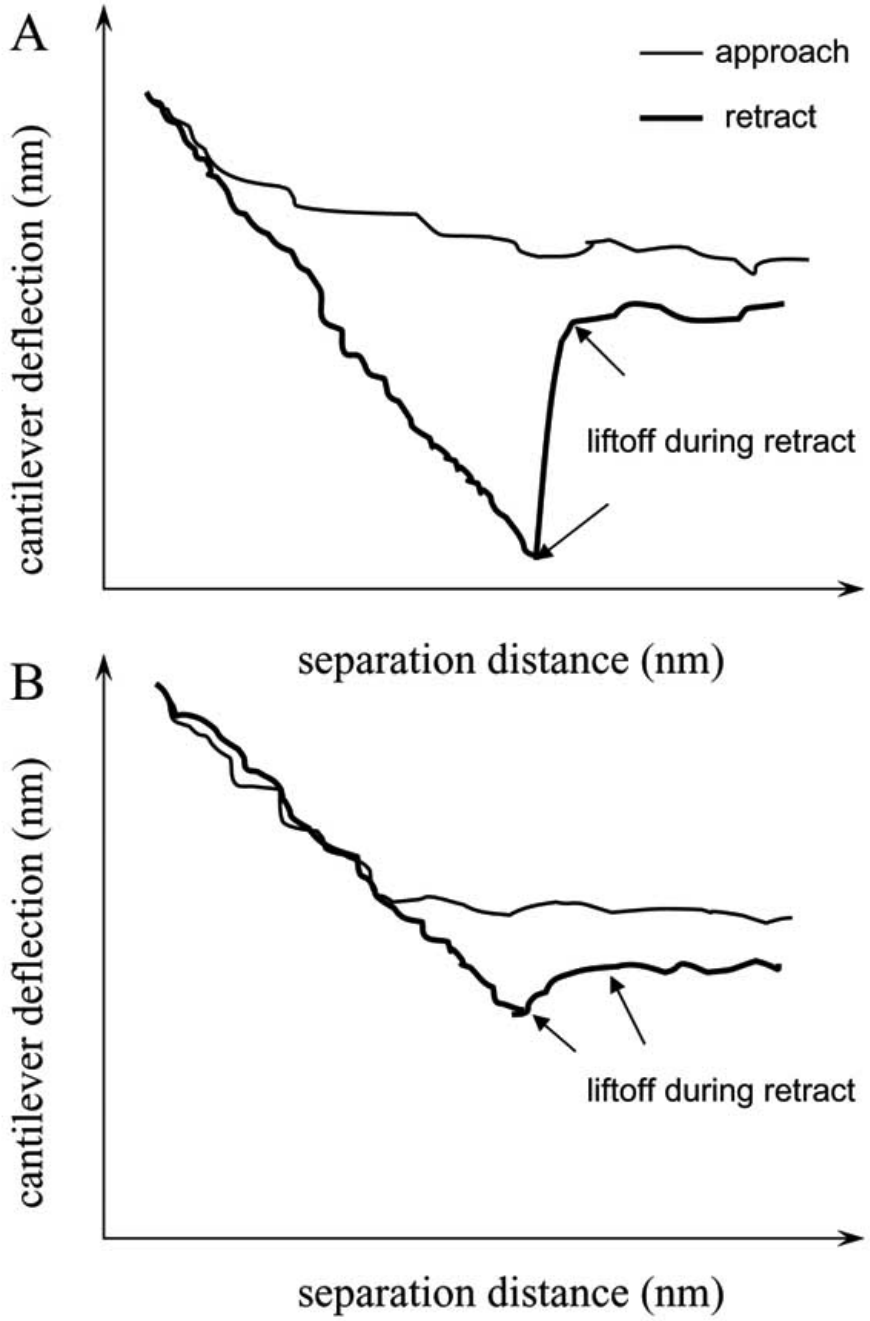

Fig. (14). Schematic representation of approach and retract force curves on a hard (A), e.g., mica, and a soft (B) sample, e.g., protein molecules. Note that the hysteresis during retract is larger on the hard sample, indicating a higher adhesion force. However, the liftoff on the soft sample is slow in comparison to the hard sample. This effect is probably due to viscous damping of the cantilever by the soft sample.

sensed through the film, even at the lowest loading forces. However, the calculated Young's modulus is only off by 50% and can thus serve as an upper estimate for the real Young's modulus. If the force sensitivity of AFM could be increased (e.g., by using softer cantilevers), then the range of thicknesses and softnesses to which a Hertzian fit can be applied could be extended.

Viscosity Map of Lysozyme Layers

Thick layers of the lysozyme were deposited on mica, and their force-distance hysteresis measured using AFM in the presence of different salts (Nemes *et al*., 1999). Sodium thiocyanate was found to increase lysozyme deformability and lower the viscosity of the protein layer, compared with sodium chloride. Sodium phosphate decreased deformability and increased the viscosity. The highest viscosity was reported to occur in the presence of phosphate. Correlating this observation with the fact that phosphate decreases the solubility of proteins, they inferred that if the main contribution to the viscosity was the friction caused by protein molecules rubbing against each other, then phosphate essentially roughened the surface. Conversely, the lowest viscosity

occurred in the presence of thiocyanate, which must therefore lubricate the surface. Detailed analysis of response-displacement curves obtained from AFM yielded estimates of the viscosity of a layer of adsorbed lysozyme due to intermolecular friction, and of intramolecular deformability. The variations of these two parameters in the presence of selected salts from the Hofmeister series were correlated with the effects of these salts on the solubility and conformational stability of the proteins.

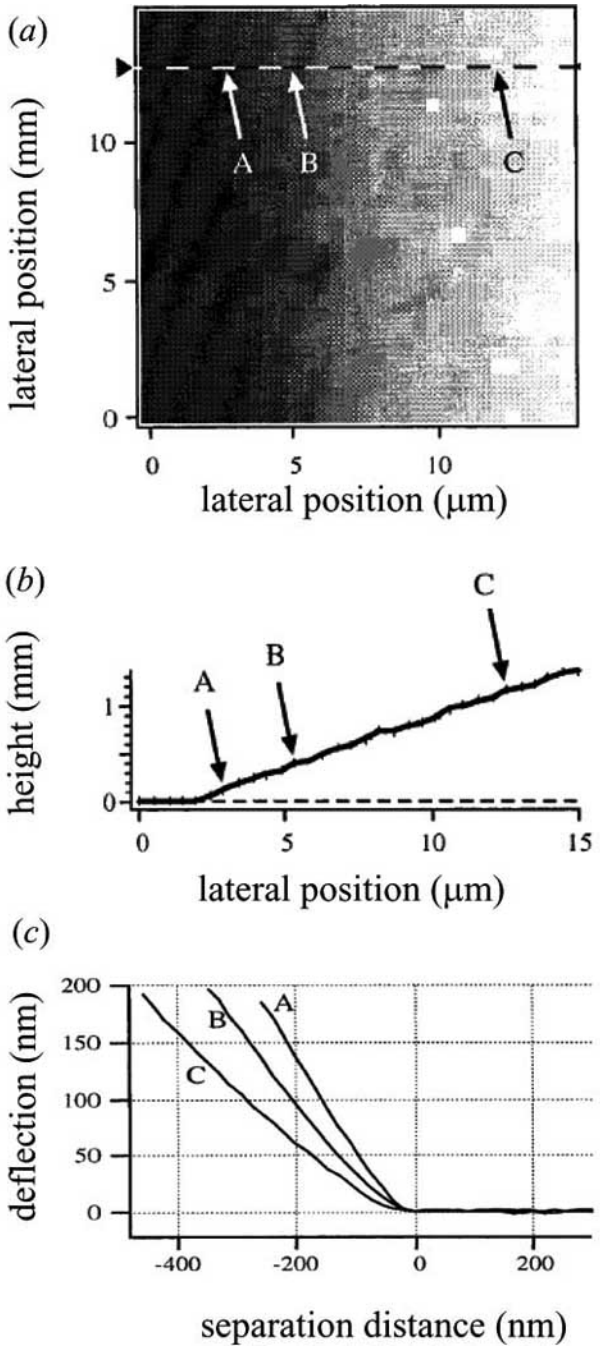

Fig. (15). (*a*) Force map of a gelatin wedge on a glass substrate. Each square in the map represents the location of one force curve. (*b*)The topography of the sample along one line of the force map is obtained by analyzing the point of contact in each force curve. (*c*) Three force curves taken at locations of a film thickness of 150 nm (curve A), 410 nm (curve B), and 1.15 μm (curve C). At high forces, the force curves are steeper for small thicknesses because the cantilever deflection is influenced by the underlying stiff substrate at these small film thicknesses. Reprinted with permission from reference (Domke *et al*., 1998). Copyright 1998 American Chemical Society.

4.3 Electrostatic Force Mapping

4.3.1 Introduction

Local electrostatic properties play a central role in a variety of biological processes. A detailed characterization of the structure and function of biological systems requires an understanding of the strength and location of their electrostatic interactions. Many techniques exist for measuring the electrostatic properties of biological molecules, such as electrophoretic, titration, electrokinetic, and redox potential measurements; however, relatively few experimental methods can determine the spatial distribution of charge on surfaces, such as membrane proteins (McLaughlin, 1989; Cevc, 1990). Cationic ferritin can label negative charges on membranes and cell surfaces and be visualized with electron microscopy (Danon *et al*., 1972). In solution, local ionic currents are measured with the vibrating probe (Jaffe and Nuccitelli, 1974) and the scanning ion-conductance microscope (Hansma *et al*., 1989). The AFM tip is sensitive to electrostatic interactions with a sample surface in solution; it can therefore provide quantitative information about surface charge densities of proteins with high spatial resolution.

Quantitative electrostatic measurements with the AFM are based on forces produced from overlapping electrical double layers as a charged probe is brought near a charged sample surface (Fig. **16**). This paradigm was initially developed for other experimental approaches, and has been particularly well utilized with the surface forces apparatus (SFA). The SFA work has shown that the Derjaguin, Landau, Verwey, and Overbeek Theory (DLVO theory) can be used to relate force measurements to surface charge (Israelachvili and Adams, 1977; Israelachvili, 1992). It has since been shown that DLVO theory can be applied to AFM measurements (Ducker *et al*., 1991). Subsequently, a number of groups have measured surface charge density and Debye length as a function of pH, electrolyte type, and concentration with the AFM and found agreement with standard DLVO theory for measurements over sample surfaces (Ducker *et al*., 1991; Hillier *et al*., 1996; Larson *et al*., 1997; Biggs and Pround, 1997). All these measurements are based on fitting force-distance curves to DLVO theory and thus require a measurement of the tip-sample separation distance.

4.3.2. Theory

Electrostatic interactions measured using AFM are most commonly covered by the continuum DLVO theory (Israelachvili, 1992). Here, the interplay between the electrostatic double layer (EDL) force (F_{ele}) and the van der Waals force (F_{vdw}) is described, neglecting effects of ion radii, hydration forces, steric forces and specific interactions (Israelachvili and Adams, 1977; Pashley, 1981; Butt, 1991b; Israelachvili, 1992). The interaction force that arises from overlapping double layers when one charged surface (an

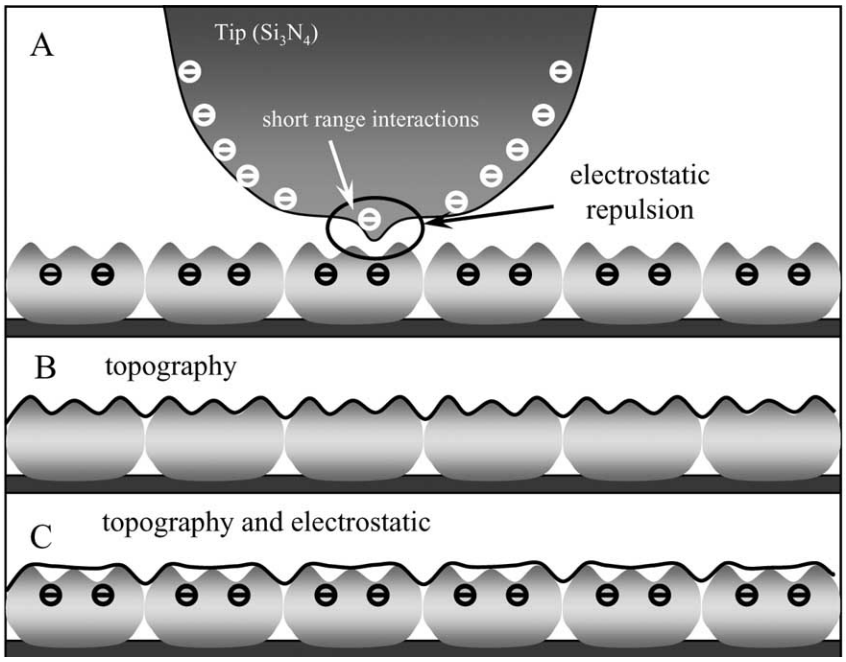

Fig. (16). Force mapping interactions between AFM tip and protein sample in buffer solution. (A) The electrostatic double-layer force interacts *via* long-range forces with a relatively large area of the protein assembly. The force effectively interacting at the AFM tip apex is a composite of all interacting forces. (B) Scanning a negatively charged AFM silicon nitride tip over an electrically neutral surface reveals the true topography. (C) In case of negative charge of protein as the sample, the AFM tip detects local electrostatic repulsions. The resulting topograph represents a mixture of height and electrostatic information.

AFM tip) is brought close enough to a second surface (e.g., protein molecules), is directly related to the charge density on or the potential of the two surfaces. While the two limits of the theory, constant charge and constant potential, diverge for small separations, they quickly converge at separations greater than several nanometers (Israelachvili, 1992). If we consider the AFM tip as a sphere and the sample as a flat plane, then the total force, F, is described by

$$F(d) = F_{ele}(d) + F_{vdw}(d) = \frac{4\pi R\lambda\sigma_p\sigma_t}{\varepsilon_e\varepsilon_0} e^{-d/\lambda} - \frac{H_a R}{6d^2} \qquad [5]$$

where R is the radius of the sphere, d the tip-sample separation distance, σ_t the surface charge density of the sphere, σ_p the surface charge density of the biomolecular plane, ε_e the dielectric constant of the medium, ε_o the permittivity of the free space, λ Debye length, and H_a is the Hamaker constant . Equation [5] holds so long as R, λ, σ_t, and σ_p do not vary significantly with d. We note that explicitly modeling the tip as an inverted pyramid instead of a sphere adds to Eq. [5] a geometrical factor independent of d that does not affect subsequent calculations (Butt, 1991b, 1992). The Debye length λ characterizes the exponential decrease of the potential resulting from screening the surface charges with electrolytes, with $\lambda = 0.304\ \text{nm}/\sqrt{C}$ for mono-valent and $0.174\ \text{nm}/\sqrt{C}$ for divalent (1:2 or 2:1) electrolytes. Hence, if the electrolyte composition and pH of the buffer solution are known, the measured exponential decay of the force can be fitted to reveal the surface charge density of the object (Israelachvili, 1992).

4.3.3. Measurement

The AFM can be used to map the spatial distribution of surface charge by (1) using isoforce images based on a repulsive double-layer force or (2) using arrays of force-distance curves. Force distance curves are used to examine the spatial distribution of surface charge density and large arrays of force curves are used to map charge distribution of biological materials. All these measurements of electrostatic force are based on fitting force-distance curves to DLVO theory and thus require an absolute measurement of the tip-sample separation distance, D. Because current AFM have no method independent of the tip-sample interaction to determine D, in practice force-distance curves have to include tip-sample contact. In this mode of electrostatic force mapping, force curves are usually taken while the AFM tip is scanned by a piezoelectric scanner across the sample.

4.3.4. Examples

The AFM probes have been used as sensors to probe charges of biological surfaces immersed in buffer solution (Butt *et al*., 1995). The electrostatic double-layer force (Israelachvili, 1992) interacting between the charged probe and charged regions of the biological sample can contribute significantly to the AFM topograph recorded (Muller and Engel, 1997; Rotsch and Radmacher, 1997) and can be tuned by the electrolyte concentration and the pH of the buffer solution. The DLVO theory describes the exponential decay of the electrostatic double-layer force as a function of the surface separation (Israelachvili, 1992). Whereas AFM probes have been used to measure the average surface charges from force-distance curves (Butt, 1991a, b; Ducker *et al*., 1991), surface charge maps have been obtained at 40-nm lateral resolution by recording force-distance curves at each pixel of the sampled surface (Rotsch and Radmacher, 1997; Heinz and Hoh, 1999b).

Electrostatic Potential Mapping of Channel-Forming Protein OmpF Porin

Philippsen and coworkers (2002) used AFM to image native transmembrane channel-forming protein OmpF porin located in the outer membrane of *E. coli* and to determine the electrostatic potential generated by the protein (Fig. **17**). The OmpF porin trimers were imaged at a lateral resolution of ~0.5 nm and a vertical resolution of ~0.1 nm at variable electrolyte concentrations of the buffer solution. Differences measured between topographs recorded at variable ionic strength allowed the electrostatic potential mapping of OmpF porin. The potential map acquired by AFM showed qualitative agreement with continuum electrostatic calculations based on the atomic OmpF porin embedded in a lipid bilayer at the same electrolyte concentrations. This method opens a novel avenue to determine the electrostatic potential of native protein surfaces at a lateral resolution better than 1 nm and a vertical resolution of ~0.1 nm.

CONCLUSION

AFM has opened an innovative approach to investigating directly the ranges and magnitudes of the interaction forces between protein and other molecules. It has also proved its value not only for resolving the topographical structure of protein samples, but also for imaging and mapping the forces that control mechanical properties of proteins under physiological conditions. In addition, it allows individual protein molecules and complexes to be stretched and disrupted for measuring the forces, which stabilize protein structure directly on a single molecule. A major advantage of AFM over other techniques is its lateral resolution which is of paramount importance at the μm and nm scale. However, AFM has the disadvantage that it is a surface technique for force measurement, implying that force is generated in only one direction. Especially in the case of rupture force measurements, this might not be the energetically mostly preferred way to separate complexes. Compared to other nanoscopic force measurement devices, such as optical and magnetic trapping and micropipettes, another disadvantage of AFM is that the hydrodynamic damping is higher than in bulk liquid, and thus the force sensitivity is intrinsically lower than those other techniques. Nevertheless, AFM might be the most suitable technique to study a variety of different biological problems, whether they are structural, molecular interactions or dynamical measurements. AFM will prove to be a valuable technique for proteomics with its own unique contributions to our comprehension of the principles of protein folding and recognition.

ACKNOWLEDGEMENT

This work was supported by MEA (Grand 92-EC-17-A-05-S1-0017) and NSC (Grand 93-2320-B-002-003 and 93-2323-B-002-013). The authors thank Dr Liang-Ping Lin and Dr Su-Ming Hsu.

ABBREVIATIONS

AFM = Atomic force microscopy

BSA = Bovine serum albumin

DLVO = Derjaguin, Landau, Verwey, and Overbeek

DSP = Digital signal processor

HV = High voltage

ICAM1 = Intercellular adhesion molecule-1

PBS = Phosphate buffered saline

pN = Piconewton

SFA = Surface forces apparatus

STM = Scanning tunneling microscopy

REFERENCES

Allen, S., Davies, J., Dawkes, A.C., Davies, M.C., Edwards, J.C., Parker, M.C., Roberts, C.J., Sefton, J., *et al*. (1996). In situ observation of streptavidin-biotin binding on an immunoassay well surface using an atomic force microscope. *FEBS Lett.* **390**: 161-4.

Allen, S., Chen, X., Davies, J., Davies, M.C., Dawkes, A.C., Edwards, J.C., Roberts, C.J., Sefton, J., *et al.* (1997). Detection of antigen-antibody binding events with the atomic force microscope. *Biochemistry* **36**: 7457-3.

Aranda-Espinoza, H., Carl, P., Leterrier, J.F., Janmey, P. and Discher, D.E. (2002). Domain unfolding in neurofilament sidearms: effects of phosphorylation and ATP. *FEBS Lett*. **531**: 397-401.

Baselt, D.R. (1994). Imaging spectroscopy with the atomic force microscope. *J. Appl. Phys.* **76**: 33-8.

Baumgartner, W., Hinterdorfer, P., Ness, W., Raab, A., Vestweber, D., Schindler, H. and Drenckhahn, D. (2000). Cadherin interaction probed by atomic force microscopy. *Proc. Natl. Acad. Sci. USA* **97**: 4005-10.

Bell, G.I. (1978). Models for the specific adhesion of cells to cells. *Science* **200**: 618-27.

Berry, M., McMaster, T.J., Corfield, A.P. and Miles, M.J. (2001). Exploring the molecular adhesion of ocular mucins. *Biomacromolecules* **2**: 498-503.

Biggs, S. and Proud, A.D. (1997). Forces between silica surfaces in aqueous solutions of a weak polyelectrolyte. *Langmuir* **13**: 7202-10.

Binnig, G., Rohrer, H., Gerber, Ch. and E. Weibel, E. (1982). Tunneling through a controllable vacuum gap. *Appl. Phys. Lett.* **40**: 178-80.

Binnig, G., Quate, C.F. and Gerber, Ch. (1986). Atomic force microscope. *Phys. Rev. Lett.* **56**: 930-3.

Braunewell, K.H. and Gundelfinger, E.D.(1999). Intracellular neuronal calcium sensor proteins: a family of EF-hand calcium-binding proteins in search of a function. *Cell Tissue Res.* **295**: 1-12.

Burnham, N.A. and Colton, R.J. (1993). In Scanning Tunneling Microscopy and Spectroscopy. (Bonnell, D.A., Ed., VCH Publisher). New York, pp 191.

Butt, H.J. (1991a). Measuring electrostatic, van der Waals, and hydration forces in electrolyte solution with an atomic force microscope. *Biophys. J.* **60**: 1438-44.

Butt, H.J. (1991b). Electrostatic interactions in atomic force microscopy. *Biophys. J.* **60**: 777-85.

Butt, H.J. (1992). Measuring local surface charge densities in electrolyte solutions with a scanning force microscope. *Biophys. J.* **63**: 578-82.

Butt, H.J., Jaschke, M. and Ducker, W. (1995). Measuring surface forces in aqueous solution with the atomic force microscope. *Bioelect. Bioenerg.* **38**: 191-201.

Cai, X.E and Yang, J. (2003). The binding potential between the cholera toxin B-oligomer and its receptor. *Biochemistry* **42**: 4028-34.

Carrion-Vazquez, M., Marszalek, P.E., Oberhauser, A.F. and Fernandez, J.M. (1999). Atomic force microscopy captures length phenotypes in single proteins. *Proc. Natl. Acad. Sci. USA* **96**: 11288-92.

Carrion-Vazquez, M., Oberhauser, A.F., Fisher, T.E., Marszalek, P.E., Li, H. and Fernandez, J.M. (2000). Mechanical design of proteins studied by single-molecule force spectroscopy and protein engineering. *Prog. Biophys. Mol. Biol.* **74**: 63-91.

Cevc, G. (1990). Membrane electrostatics. *Biochim. Biophys. Acta* **1031**: 311–82.

Chen, A. and Moy, V.T. (2000). Cross-linking of cell surface receptors enhances cooperativity of molecular adhesion. *Biophys. J.* **78**: 2814-20.

Chen, C.H., Vesecky, S.M. and Gewirth, A.A. (1992). In situ atomic force microscopy of underpotential deposition of silver on gold(111). *J. Am. Chem. Soc*. **114**: 451-8.

Chilkoti, A., Boland, T., Ratner, B.D. and Stayton, P.S. (1995). The relationship between ligand-binding thermodynamics and protein-

ligand interaction forces measured by atomic force microscopy. *Biophys. J.* **69**: 2125-30.

Chothia, C. and Jones, E.Y. (1997). The molecular structure of cell adhesion molecules. *Annu. Rev. Biochem.* **66**: 823-62.

Cleveland, J.P., Manne, S., Bocek, D. and Hansma, P.K. (1993) A nondestructive method for determining the spring constant of cantilevers for scanning force microscopy. *Rev. Sci. Instru.* **64**: 403-5.

Creuzet, F., Ryschenkow, G. and Arribart, H. (1992). *J. Adhes.* **40**: 15-22.

Dammer, U., Popescu, O., Wagner, P., Anselmetti, D., Guntherodt, H.J. and Misevic, G.N. (1995a) Binding strength between cell adhesion proteoglycans measured by atomic force microscopy. *Science* **267**: 1173-5.

Dammer, U., Anselmetti, D., Dreier, M., Hegner, M., Huber, W., Hurst, J., Misevic, G. and Guntherodt, H.J. (1995b) In *Forces in Scanning Probe Methods*, Guntherodt, H.J., Ed.; Kluwer Academic Publishers: Dordrecht, The Netherlands, pp 625.

Dammer, U., Hegner, M., Anselmetti, D., Wagner, P., Dreier, M., Huber, W. and Guntherodt, H.J. (1996). Specific antigen/antibody interactions measured by force microscopy. *Biophys. J.* **70**: 2437-41.

Danon, D., Goldstein, L., Marikovsky, Y. and Skutelsky, E. (1972). Use of cationized ferritin as a label of negative charges on cell surfaces. *J. Ultrastruct. Res.* **38**: 500-10.

Davis, D.R. and Padlan, E.A. (1990). Antibody-antigen complexes. *Annu. Rev. Biochem.* **59**: 439-73.

Desmeules, P., Grandbois, M., Bondarenko, V.A., Yamazaki, A. and Salesse, C. (2002). Measurement of Membrane Binding between Recoverin, a Calcium-Myristoyl Switch Protein, and Lipid Bilayers by AFM-Based Force Spectroscopy. *Biophys. J.* **82**: 3343-50.

Dettmann, W., Grandbois, M., Andre, S., Benoit, M., Wehle, A.K., Kaltner, H., Gabius, H.J. and Gaub, H.E. (2000). Differences in zero-force and force-driven kinetics of ligand dissociation from beta-galactoside-specific proteins (plant and animal lectins, immunoglobulin G) monitored by plasmon resonance and dynamic single molecule force microscopy. *Arch. Biochem. Biophys.* **383**: 157-70.

Dizhoor A.M., Ray, S., Kumar, S., Niemi, G., Spencer, M., Brolley, D., Walsh, K.A., Philipov, P.P., *et al*. (1991). Recoverin: a calcium sensitive activator of retinal rod guanylate cyclase. *Science* **22**: 915-8.

Domke, J. and Radmacher, M. (1998). Measuring the elastic properties of thin polymer films with the atomic force microscope. *Langmuir* **14:** 3320-5.

Ducker, W.A., Senden, T.J. and Pashley, R.M. (1991). Direct measurement of colloidal forces using an atomic force microscope. *Nature* **353**: 239-41.

Ducker, W.A., Senden, T.J. and Pashley, R.M. (1992). Measurement of forces in liquids using a force microscope. *Langmuir* **8**: 1831-6.

Evans, E., Berk, D. and Leung, A. (1991). Detachment of agglutinin-bonded red blood cells. Forces to rupture molecular-point attachments. *Biophys. J.* **59**: 838-48.

Evans, E., Ritchie, K. and Merkel, R. (1995). Sensitive force technique to probe molecular adhesion and structural linkages at biological interfaces. *Biophys. J.* **68**: 2580-7.

Florin, E.L., Moy, V.T. and Gaub, H.E. (1994). Adhesion forces between individual ligand-receptor pairs. *Science* **264**: 415-7.

Florin, E.-L., Rief, M., Lehmann, H., Ludwig, M., Dornmair, C., Moy, V. T. and Gaub, H. E. (1995). Sensing specific molecular interactions with the atomic force microscope. *Biosens. Bioelectron.* **10**: 895.

Frauenfelder, H., Sligar, S.G. and Wolynes, P.G. (1991). The energy landscapes and motions of proteins. *Science* **254**:1598-1603.

Fritz, M., Radmacher, M., Petersen, N. and Gaub, H.E. (1994). Visualization and identification of intracellular structures by force modulation microscopy and drug induced degradation. *J. Vac. Sci. Technol. B.* **12**: 1526-9.

Fritz, J., Anselmetti, D., Jarchow, J. and Fernandez-Busquets, X. (1997). Probing single biomolecules with atomic force microscopy. *J. Struct. Biol.* **119**: 165-71.

Fritz, J., Katopodis, A.G., Kolbinger, F. and Anselmetti, D. (1998). Force-mediated kinetics of single P-selectin/ligand complexes observed by atomic force microscopy. *Proc. Natl. Acad. Sci. USA* **95**: 12283-8.

Fritzsche, W. and Henderson, E. (1997). Mapping elasticity of rehydrated metaphase chromosomes by scanning force microscopy. *Ultramicroscopy* **69**: 191-200.

Fung, Y. C. (1993). "Biomechanics – Mechanical properties of living tissues." , 2nd ed..Springer, New York.

Furuike, S., Ito, T. and Yamazaki, M. (2001). Mechanical unfolding of single filamin A (ABP-280) molecules detected by atomic force microscopy. *FEBS Lett.* **498**: 72-5.

Guckenberger, R., Heim, M., Cevc, G., Knapp, H.F., Wiegrabe, W. and Hillebrand, A.(1994). Scanning tunneling microscopy of insulators and biological specimens based on lateral conductivity of ultrathin water films. *Science* **266**: 1538-40.

Hansma, P.K., Drake, B., Marti, O., Gould, S.A.C. and Prater, C.B. (1989). The scanning ion-conductance microscope. *Science* **243**: 641-3.

Heinz, W.F. and Hoh, J.H. (1999a). Spatially resolved force spectroscopy of biological surfaces using the atomic force microscope. *Trends Biotechnol.* **17**: 143-50.

Heinz, W.F. and Hoh, J.H. (1999b). Relative surface charge density mapping with the atomic force microscope. *Biophys. J.* **76**: 528-38.

Hertadi, R. and Ikai, A. (2002). Unfolding mechanics of holo- and apocalmodulin studied by the atomic force microscope. *Protein Sci.* **11**: 1532-8.

Hertz, H. (1882). Uber die Beruhrung fester elastischer Korper. J. Reine Angew. *Mathematik* **92**: 156-71.

Hillier, A.C., Kim, S. and Bard, A.J. (1996). Measurement of double-layer forces at the electrode/electrolyte interface using the atomic force microscope: potential and anion dependent interactions. *J. Phys. Chem.* **100**: 18808-17.

Hinterdorfer, P., Baumgartner, W., Gruber, H.J., Schilcher, K. and Schindler, H. (1996). Detection and localization of individual antibody-antigen recognition events by atomic force microscopy. *Proc. Natl. Acad. Sci. USA* **93**: 3477-81.

Hoh, J.H. and Schoenenberger, C.A. (1994). Surface morphology and mechanical properties of MDCK monolayers by atomic force microscopy. *Biophys. J.* **107**: 1105-14.

Hutter, J.L. and Bechhoefer, J. (1994). Calibration of atomic force microscope tips. *Rev. Sci. Instrum.* **64**: 1868-73.

Ishijima, Kojima, H., Higuchi, H., Harada, Y., Funatsu, T. and Yanagida, T. (1996). Multiple- and single-molecule analysis of the actomyosin motor by nanometer-piconewton manipulation with a microneedle: unitary steps and forces. *Biophys. J.* **70**: 383-400.

Israelachvili, J. and Adams, G. (1977). Measurement of forces between two mica surfaces in aqueous electrolyte solutions in the range 0-100 nm. *J. Chem. Soc. Faraday Trans. I.* **74**: 975-1000.

Israelachvili, J. (1992). Intermolecular and surface forces. Academic Press Limited, London. pp. 213-254.

Jaffe, L.F. and Nuccitelli, R. (1974). An ultrasensitive vibrating probe for measuring steady extracellular currents. *J Cell Biol.* **63**: 614-28.

Kiridena, W., Jain, V., Kuo, P.K. and Liu, G.Y. (1997). Nanometer-scale Elasticity Measurements on Organic Monolayers Using Scanning Force Microscopy. *Surf. Interface Anal.* **25**: 383-9.

Kuo, S. and Sheetz, M. (1993). Force of Single Kinesin Molecules Measured With Optical Tweezers. *Science* **260**: 232-4.

Larson, I., Drummond, C.J., Chan, D.Y.C. and Grieser, F. (1997). Direct force measurements between silica and alumina. *Langmuir* **13**: 2109-12.

Law, R., Carl, P., Harper, S., Dalhaimer, P., Speicher, D.W. and Discher, D.E. (2003). Cooperativity in forced unfolding of tandem spectrin repeats. *Biophys. J.* **84**: 533-44.

Lee, G..U., Kidwell, D.A. and Colton, R.J. (1994a). Sensing Discrete Streptavidin-Biotin Interactions with Atomic Force Microscopy. *Langmuir* **10**: 354-7.

Lee, G.U., Chrisey, L.A. and Colton, R.J. (1994b). Direct measurement of the forces between complementary strands of DNA. *Science* **266**: 771-3.

Lehenkari, P.P. and Horton, M.A. (1999). Single integrin molecule adhesion forces in intact cells measured by atomic force microscopy. *Biochem. Biophys. Res. Commun.* **259**: 645-50.

Ludwig, M., Dettmann, W. and Gaub, H.E. (1997). Atomic force microscope imaging contrast based on molecular recognition. *Biophys. J.* **72**:445-8.

Marshall, B.T., Long, M., Piper, J.W., Yago, T., McEver, R.P. and Zhu, C. (2003). Direct observation of catch bonds involving cell-adhesion molecules. *Nature* **423**: 190-3.

Marszalek, P.E., Lu, H., Li, H., Carrion-Vazquez, M., Oberhauser, A.F., Schulten, K. and Fernandez, J.M. (1999). Mechanical unfolding intermediates in titin modules. *Nature* **402**: 100-3.

McEver, R.P., Moore, K.L. and Cummings, R.D. (1995). Leukocyte trafficking mediated by selectin-carbohydrate interactions. *J. Biol. Chem.* **270**: 11025-8.

McLaughlin, S. (1989). The electrostatic properties of membranes. *Annu. Rev. Biophys. Biophys. Chem.* **18**: 113-36.

Melander, W. and Horvath, C. (1977). Salt effect on hydrophobic interactions in precipitation and chromatography of proteins: an

interpretation of the lyotropic series. *Arch. Biochem. Biophys.* **183**: 200-15.

Misevic, G.N., Finne, J. and Burger, M.M. (1987). Involvement of carbohydrates as multiple low affinity interaction sites in the self-association of the aggregation factor from the marine sponge Microciona prolifera. *J. Biol. Chem.* **262**: 5870-80.

Mitsui, K., Hara, M. and Ikai, A. (1996). Mechanical unfolding of 2-macroglobulin molecules with atomic force microscope. *FEBS Lett.* **385**: 29-33.

Miyata, H., Yasuda, R. and Kinosita, Jr. K. (1996). Strength and lifetime of the bond between actin and skeletal muscle alpha-actinin studied with an optical trapping technique. *Biochim. Biophys. Acta.* **1290**: 83-8.

Mizes, H.A., Loh, K.G., Miller, R.J.D., Ahuja, S.K. and Grabowski, E.F. (1991). Submicron probe of polymer adhesion with atomic force microscopy: Dependence on topography and material inhomogeneities. *Appl. Phys. Lett.* **59**: 2901-12.

Moller, C., Fotiadis, D., Suda, K., Engel, A., Kessler, M. and Muller, D.J. (2003). Determining molecular forces that stabilize human aquaporin-1. *J. Struct. Biol.* **142**: 369-78.

Morris, V.J., Kirby, A.R. and Gunning, A.P. (1999). Atomic force microscopy for biologists. Imperial College Press, London, UK.

Moy, V.T., Florin, E.L. and Gaub, H.E. (1994a). Intermolecular forces and energies between ligands and receptors. *Science* **266**: 257-9.

Moy, V.T., Florin, E.L. and Gaub, H.E. (1994b). Adhesive forces between ligand and receptor measured by AFM. *Colloid Surf.* **A 93**: 343-8.

Müller, D.J. and Engel, A. (1997). The height of biomolecules measured with the atomic force microscope depends on electrostatic interactions. *Biophys. J.* **73**: 1633-44.

Mueller, H., Butt, H.J. and Bamberg, E. (1999). Force measurements on myelin basic protein adsorbed to mica and lipid bilayer surfaces done with the atomic force microscope. *Biophys. J.* **76**: 1072-9.

Nakajima, H., Kunioka, Y., Nakano, K., Shimizu, K., Seto., M. and Ando, T. (1997). Scanning force microscopy of the interaction events between a single molecule of heavy meromyosin and actin. *Biochem. Biophys. Research Communication* **234**: 178-82.

Nemes, C., Rozlosnik, N. and Ramsden, J.J. (1999).Direct measurement of the viscoelasticity of adsorbed protein layers using atomic force microscopy. *Phys. Rev. E. Stat. Phys. Plasmas Fluids Relat. Interdiscip Topics.* **60**: 1166-9.

Nicklas, R. B. (1983). Measurements of the force produced by the mitotic spindle in anaphase. *J. Cell Biol.* **97**: 542-8.

Oberhauser, A.F., Marszalek, P.E., Erickson, H.P. and Fernandez, J.M. (1998). The molecular elasticity of the extracellular matrix protein tenascin. *Nature* **393**: 181-5.

Oberhauser, A.F., Hansma, P.K., Carrion-Vazquez, M. and Fernandez, J.M. (2001). Stepwise unfolding of titin under force-clamp atomic force microscopy. *Proc. Natl. Acad. Sci. USA* **98**: 468-72.

Oroudjev, E., Soares, J., Arcdiacono, S., Thompson, J.B., Fossey, S.A. and Hansma, H.G. (2002). Segmented nanofibers of spider dragline silk: atomic force microscopy and single-molecule force spectroscopy. *Proc. Natl. Acad. Sci. USA* **99**(Suppl 2): 6460-5.

Osada, T., Itoh, A. and Ikai, A. (2003). Mapping of the receptor-associated protein (RAP) binding proteins on living fibroblast cells using an atomic force microscope. *Ultramicroscopy* **97**: 353-7.

Parsegian, V.A., Rand, R.P., Fuller, N.L. and Rau, D.C. (1986). Osmotic stress for the direct measurement of intermolecular forces. *Methods Enzymol.* **127**: 400-16.

Pashley, R. M. (1981). DLVO and hydration forces between mica surfaces in Li, Na, K and Cs electrolyte solutions: a correlation of double-layer and hydration forces with surface cation exchange properties. *J. Colloid. Interface Sci.* **83**: 531-46.

Philippsen, A., Im, W., Engel, A., Schirmer, T., Roux, B. and Muller, D.J.(2002). Imaging the electrostatic potential of transmembrane channels: atomic probe microscopy of OmpF porin. *Biophys. J.* **82**: 1667-76.

Pierce, M., Stuart, J., Pungor, A., Dryden, P. and Hlady, V. (1994a). Adhesion forces measurements using an atomic force microscope upgraded with a linear position sensitive detector. *Langmuir* **10**: 3217-21.

Pierce, M.L., Stuart, J.K., Pungor, A., Dryden, P. and Hlady, V. (1994b). Specific and non-specific adhesion force measurements using AFM with a linear position sensitive detector. *Langmuir* **10**: 3217-26.

Pierres, A., Benoliel, A.M. and Bongrand, P. (1996). Measuring bonds between surface-associated molecules. *Journal of Immunological Methods* **196**: 105-20.

Politou, A.S., Thomas, D.J. and Pastore, A. (1995). The folding and stability of titin immunoglobulin-like modules, with implications for the mechanism of elasticity. *Biophys. J.* **69**:2601-10.

Popescu, O., Checiu, I., Gherghel, P., Simon, Z. and Misevic, G.N. (2003). Quantitative and qualitative approach of glycan-glycan interactions in marine sponges. *Biochimie.* **85**: 181-8.

Putman, C.A., van der Werf, K.O., de Grooth, B.G., van Hulst, N.F. and Greve, J. (1994). Viscoelasticity of living cells allows high resolution imaging by tapping mode atomic force microscopy. *Biophys. J.* **67**: 1749-53.

Radmacher, M., Tillman, R.W., Fritz, M. and Gaub, H.E. (1992). From molecules to cells: imaging soft samples with the atomic force microscope. *Science* **257**: 1900-5.

Radmacher, M., Tillman, R.W. and Gaub, H.E. (1993). Imaging viscolasticity by force modulation with the atomic force microscope. *Biophys. J.* **64**: 735-42.

Radmacher, M., Fritz, M., Cleveland, J.P., Walters, D.R. and Hansma, P.K. (1994). Imaging adhesion forces and elasticity of lysozyme adsorbed on mica by atomic force microscopy. *Langmuir* **10**: 3809-14.

Radmacher, M., Fritz, M. and Hansma, P. K. (1995). Imaging soft samples with the atomic force microscope: gelatin in water and propanol. *Biophys. J.* **69**: 264-70.

Radmacher, M., Fritz, M., Kacher, C.M., Cleveland, J.P. and Hansma, P.K. (1996). Measuring the viscoelastic properties of human platelets with the atomic force microscope. *Biophys. J.* **70**: 556-67.

Radmacher, M. (2002). Measuring the elastic properties of living cells by the atomic force microscope. *Methods in Cell Biology* **68**: 67-90.

Rief, M., Gautel, M., Oesterhelt, F., Fernandez, J.M. and Gaub, H.E. (1997). Reversible unfolding of individual titin immunoglobulin domains by AFM. *Science* **276**: 1109-12.

Rief, M., Gautel, M., Schemmel, A. and Gaub, H.E. (1998). The mechanical stability of immunoglobulin and fibronectin III domains in the muscle protein titin measured by atomic force microscopy. *Biophys. J.* **75**: 3008-14.

Rief, M., Pascual, J., Saraste, M. and Gaub, H.E. (1999). Single molecule force spectroscopy of spectrin repeats: low unfolding forces in helix bundles. *J. Mol. Biol.* **286**: 553-61.

Ros, R., Schwesinger, F., Anselmetti, D., Kubon, M., Schafer, R., Pluckthun, A. and Tiefenauer, L. (1998). Antigen binding forces of individually addressed single-chain Fv antibody molecules. *Proc. Natl. Acad. Sci. USA* **95**: 7402-5.

Rotsch, C. and Radmacher, M. (1997). Mapping local electrostatic forces with the atomic force microscope. *Langmuir* **13**: 2825-32.

Samori, B., Siligardi, G., Quagliariello, C., Weisenhorn, A.L., Vesenka, J. and Bustamante, C.J. (1993). Chirality of DNA supercoiling assigned by scanning force microscopy. *Proc. Natl. Acad. Sci. USA* **90**: 3598-601.

Senden, T.J. and Ducker, W.A. (1994). Experimental determination of spring constants in atomic force microscopy. *Langmuir* **10**: 1003-4.

Shao, Z., Mou, J., Czajkowsky, D.M., Yang, J. and Yuan, J.Y. (1996). Biological atomic force microscopy: what is achieved and what is needed. *Advances in Physics* **45-1**: 1-86.

Sneddon, I.N. (1965). The relation between load and penetration in the axisymmetric Boussinesq problem for a punch of arbitrary profile. *Int. J. Eng. Sci.* **3**: 47-57.

Stuart, J.K. and Hlady, V. (1995). Effects of discrete protein-surface interactions in scanning force microscopy adhesion force measurements. *Langmuir* **11**: 1368-74.

Svoboda, K. and Block, S.M. (1994). Biological Applications of Optical Forces. *Ann. Rev. Biophys. Biomol. Struct.* **23:** 247-85.

Tao, N.J., Lindsay, N.M. and Lees, S. (1992). Measuring the microelastic properties of biological materials. *Biophys. J.* **63**: 1165-9.

Timoshenko, S.P. and Goodier, J.N. (1970). Theory of elasticity, McGraw-Hill, 3rd ed. New York.

Treloar, L.R. (1975). The Physics of Rubber Elasticity, 3rd ed. Clarendon Press, Oxford, pp. 72-77.

Van Oss, C.J. (1994). Nature of specific ligand-receptor bonds, in particular the antigen-antibody bond. In Immunochemistry. (Van Oss, C.J. and van Regenmortel, H.V., editors). Marcel Dekker, New York, pp 581-614.

Vinckier, A., Dumortier, C., Engelborghs, Y. and Hellemans, L., (1996). Dynamic and mechanistic study immobilized microtubules with atomic force microscopy. *J. Vac. Sci. Technol. B.* **14:** 1427-31.

Vinckier, A., Gervasoni, P., Zaugg, F., Ziegler, U., Lindner, P. and Groscurth (1998). Atomic force microscopy detects changes in the

interaction forces between GroEL and substrate proteins. *Biophys. J.* **74**: 3256-63.

Vinckier, A. and Semenza, G. (1998). Measuring elasticity of biological materials by atomic force microscopy. *FEBS Letters* **430**: 12-6.

Webster, D.M., Henry, A.H. and Rees, A.R. (1994). Antibody-antigen interactions. *Curr. Opin. Struct. Biol.* **4**: 123-9.

Wong, S.S., Joselevich, E., Woolley, A.T., Cheung, C.L. and Lieber, C.M. (1998). Covalently functionalized nanotubes as nanometre-sized probes in chemistry and biology. *Nature* **394:** 52-5.

Willemsen, O.H., Snel, M.M.E., van der Werf, K.O., de Grooth, B.G., Greve, J., Hinterdorfer, P., Gruber, H.J., Schindler, H., *et al*. (1998). Simultaneous height and adhesion imaging of antibody-antigen interactions by atomic force microscopy. *Biophys. J.* **75**: 2220-8.

Willemsen, O.H., Snel, M.M.E., Cambi, A., Greve, J., De Grooth, B.G. and Figdor, C.G. (2000). Biomolecular interactions measured by atomic force microscopy. *Biophys. J.* **79**: 3267-81.

Yip, C.M., Yip, C.C. and Ward, M.D. (1998). Direct force measurements of insulin monomer-monomer interactions. *Biochemistry* **37**: 5439-49.

Yang, G., Cecconi, C., Baase, W.A., Vetter, I.R., Breyer, W.A., Haack, J.A., Matthews, B.W., Dahlquist, F.W. *et al*. (2000). Solid-state synthesis and mechanical unfolding of polymers of T4 lysozyme. *Proc. Natl. Acad. Sci. USA* **97**: 139-44.

Yuan, C., Chen, A., Kolb, P. and Moy, V.T. (2000). Energy landscape of streptavidin-biotin complexes measured by atomic force microscopy. *Biochemistry* **39**: 10219-23.

Zelatanova, J., Lindsay, S.M. and Leuba, S.H. (2000). Single molecule force spectroscopy in biology using the atomic force microscope. *Prog. Biophys. Mol. Biol.* **74**: 37-61.

Zhang, X., Wojcikiewicz, E. and Moy, V.T. (2002). Force spectroscopy of the leukocyte function-associated antigen-1/intercellular adhesion molecule-1 interaction. *Biophys. J.* **83**: 2270-9.

Received: August 20, 2003 **Accepted: February 23, 2005**